

FLUID CHARACTERIZATION USING A TEM
TRANSMISSION LINE

By

ROBERT MICHAEL TAYLOR

Bachelor of Science

Oklahoma State University

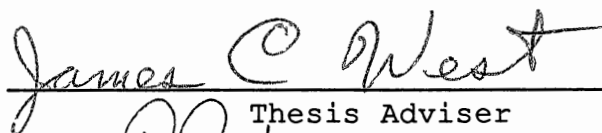
Stillwater, Oklahoma

1981


Submitted to the Faculty of the
Graduate College of the
Oklahoma State University
in partial fulfillment of
the requirements for
the Degree of
MASTER OF SCIENCE
December, 1992

FLUID CHARACTERIZATION USING A TEM
TRANSMISSION LINE


Thesis Approved:



Thesis Adviser







Dean of the Graduate College

ACKNOWLEDGMENTS

I would like to thank Dr. J. West for the advice and guidance given during the preparation of this thesis. I would also like to thank my wife Candy for her support, time, and efforts on the preparation of the text.

TABLE OF CONTENTS

Chapter	Page
I. INTRODUCTION	1
II. MEASUREMENT SYSTEM REQUIREMENTS	4
Introduction	4
Physical Size	4
Fluid Salinity/Hydrocarbon Volume Range	5
Operating Conditions	6
III. MEASUREMENT SYSTEM OVERVIEW	8
IV. MEASUREMENT SYSTEM ANALYSIS	9
Introduction	9
Homogeneous Line Plane Wave Model	9
Attenuation Response	11
Phase Shift Response	15
Coaxial Line Characteristic Impedance	18
V. NETWORK ANALYZER MEASUREMENTS	20
Introduction	20
Characteristic Impedance Set Up	20
Results and Comparison	25
Slotted Line Set Up	25
Results and Comparison	34
VI. CHOOSING PROTOTYPE SPECIFICATIONS	35
Introduction	35
Geometry	36
Operating Frequency	37

Chapter	Page
VII. PROTOTYPE ELECTRONICS CONSTRUCTION	39
Introduction	39
Flowtube	40
Transmitter	41
Local Oscillator	46
Mixer	48
Intermediate Frequency Amp	50
Phase Detector	52
Amplitude Detectors	54
Automatic Gain Control	56
Assembled System	58
VIII. PROTOTYPE TESTING	61
Introduction	61
Phase and Attenuation Measurements	62
Oil Volume Measurements	66
IX. CONCLUSIONS AND COMMENTS	74
LITERATURE CITED	76

LIST OF FIGURES

Figure	Page
1. Attenuation vs Conductivity	13
2. Effects of Relative Permeability on Attenuation	14
3. Phase Shift vs Conductivity	16
4. Effects of Relative Permeability on Phase Shift	17
5. Line Characteristic Impedance Magnitude vs Conductivity	19
6. Characteristic Impedance Measurement Set Up	22
7. Measured vs Calculated Characteristic Impedance; 115 Mhz	23
8. Measured vs Calculated Characteristic Impedance; 50 Mhz	24
9. Attenuation Measurement Set Up	27
10. Measured vs Calculated Attenuation; 200 Mhz	28
11. Measured vs Calculated Attenuation; 150 Mhz	29
12. Measured vs Calculated Attenuation; 100 Mhz	30
13. Measured vs Calculated Phase Shift; 200 Mhz	31
14. Measured vs Calculated Phase Shift; 150 Mhz	32
15. Measured vs Calculated Phase Shift; 100 Mhz	33
16. Measurement System Block Diagram	43
17. Flowtube Measurement Chamber	44
18. Transmitter Schematic	45
19. Local Oscillator Schematic	47
20. Mixer Schematic	49

Figure	Page
21. Intermediate Frequency Amplifier Schematic	51
22. Phase Detector Schematic	53
23. Amplitude Detector Schematic	55
24. Automatic Gain Control Schematic	57
25. Measurement System Photograph	59
26. Measurement System Layout	60
27. Attenuation for Final Flowtube Assembly	64
28. Phase Shift for Final Flowtube Assembly	65
29. Measured Attenuation Verses Oil Volume (11.15 mho/m) ..	68
30. Measured Phase Shift Verses Oil Volume (11.15 mho/m) ..	69
31. Measured Attenuation Verses Oil Volume (10.0 mho/m) ...	70
32. Measured Phase Shift Verses Oil Volume (10.0 mho/m) ...	71
33. Measured Attenuation Verses Oil Volume (2 mho/m)	72
34. Measured Phase Shift Verses Oil Volume (2 mho/m)	73

CHAPTER I

INTRODUCTION

Wireline formation testing is a process where a formation testing device is lowered into an open wellbore and positioned adjacent to the geological formation of interest. The device then seats a packer against the formation wall and forces a fluid extraction tube through the packer into the formation. Formation pressure is measured and a sample of formation fluids is then extracted. Tool power and communication with surface telemetry is accomplished with a seven conductor wireline. Formation fluid samples are usually taken from points in the well in which previously recorded electrical logs indicate the possibility of hydrocarbons. Several liters of fluid are typically taken. Currently, the composition of these fluid samples cannot be determined until the device is returned to surface.

A well that has been drilled for the purpose of producing hydrocarbons typically consists of a hole that is cylindrical in nature with a diameter ranging from a few inches to tens of inches and a depth below the earth's surface ranging from a few hundred to tens of thousands of feet. After drilling has been completed, electronic measurement devices are lowered into the well to record rock

and fluid properties as a function of well depth for use in predicting the presence of hydrocarbons. Among these instruments is the formation testing device which is capable of extracting fluid samples from subsurface formations penetrated by the wellbore. A measurement technique has been developed to characterize a fluid sample in situ for fluid conductivity and, in some cases, hydrocarbon volume.

Numerous methods for measuring complex permittivity of fluids have been documented. These methods can typically be classified as transmission, resonance, or reflection in nature. Resonance type methods typically consist of measuring the quality factor of the cavity (Q) and the resonant frequency of the cavity when filled with the fluid (8, 9, 10). This type of measurement is not well suited to extremely high conductivity measurements because the Q of the cavity becomes very small. Reflection methods depend on a changing reflection coefficient or voltage standing wave ratio as a lossy material is introduced as a line load or discontinuity (3, 12, 13). Again, this method yields poor accuracy for very high conductivities. Transmission type measurements where the lossy medium is substituted for some portion of the transmission line dielectric give the best results for high conductivity materials (7, 14, 15). Here, a new measurement system using the transmission technique is designed and a prototype is constructed and tested. In this system, fluid flows between the inner and outer conductors of a coaxial transmission line while the phase shift and

attenuation between two points on the line is monitored. The measurement system performs in situ conductivity measurements under dynamic fluid flow conditions. Chapter Two introduces the measurement system specifications and Chapter Three gives a measurement system overview. Chapter Four presents a TEM wave analysis of the phase shift and attenuation for a lossy coaxial line. Chapter 5 presents a comparison of measurements made using a network analyzer and a fluid filled coaxial line to the plane wave analysis of Chapter Four. In Chapter 6 the results of the network analyzer measurements are analyzed to choose the operating frequency and geometry of the prototype measurement system. Chapter 7 outlines the mechanical and electrical construction of the prototype measurement system and Chapter 8 presents the results of the testing of the measurement system.

CHAPTER II

MEASUREMENT SYSTEM REQUIREMENTS

Introduction

The measurement system requirements are those typical of wireline logging environments. The specifications are tabulated and discussed here.

Specifications

- * Flowtube length less than 3 inches
- * Flowtube diameter less than 0.3 inches
- * Fluid salinity range 250 ppm to 250,000 ppm sodium chloride
- * Hydrocarbon volumes 0-100 percent
- * Measurement to be made under dynamic fluid flow conditions
- * Circuit techniques consistent with operating temperatures of 350°F where possible.

Physical Size

The measurement system is to be utilized as an integral part of a formation testing system. Typical formation testing systems consist of a cylindrical housing less than four inches in outside diameter and tens of feet in length. This housing contains electronics, pumps, hydraulics, and

fluid sample holding chambers. Therefore, the physical size must be held to the minimum necessary to obtain a viable measurement. The size limitation must be met by both the measurement flowtube and the electronics. The measurement tube length should not exceed three inches and the flowtube inside diameter should not to exceed 0.3 inches. Flowtube inside diameters greater than 0.3 inches could possibly adversely affect sample flow characteristics. The electronics should also be kept as small as possible, although the first concern will be to provide a repeatable accurate measurement. An electronics package smaller than 3 inches by 3 inches, achieved using hybrid packaging techniques, would be ideal.

Fluid Salinity/Hydrocarbon Volume

A fluid salinity range of 250 ppm to 250,000 ppm of sodium chloride must be measurable. The approximate relationships given below relate parts per million of sodium chloride in water to the solution resistivity in ohm meters and relate the water conductivity to changes in temperature [1]

$$R_{w75} = .0123 + \frac{3647.5}{[\text{PPM (NaCl)}]^{.995}} \quad \text{EQ. (1)}$$

R_{w75} = Water resistivity at 75°F

PPM(NACL) = Parts per million sodium chloride

$$R_{w2} = R_{w1} \left(\frac{T_1 + 6.77}{T_2 + 6.77} \right) \quad \text{EQ. (2)}$$

T_1 = Temperature 1 in degrees Fahrenheit

T_2 = Temperature 2 in degrees Fahrenheit

R_{w2} = Fluid resistivity at temperature two

R_{w1} = Fluid resistivity at temperature one

Using these conversions with the given salinity range and temperatures from 72°F (room temperature) to 350°F, the operating conductivity will range from 0.5 mhos to 115 mhos per meter. The system should also be capable of measuring the conductivity of fluids ranging from zero to 100 percent hydrocarbons. Increasing the hydrocarbon content of a fluid sample will decrease the measured conductivity and dielectric constant.

Operating Conditions

The primary stipulations on operating conditions concern temperature and dynamic fluid flow. The geometry of the

measurement sensor is to be such that fluids can be characterized as they flow through the device from the intake to the sample chamber. No formal requirement for the electronics operating temperature has been established, although use of electronic techniques known to work in excess of 350°F is preferred.

CHAPTER III

MEASUREMENT SYSTEM OVERVIEW

The purpose of the measurement system is to provide a means of continuously monitoring fluid conductivity and prediction of hydrocarbon content. This is accomplished by measuring the phase shift and attenuation between two points on a coaxial line in which the fluid under investigation fills the space between inner and outer conductors.

With fluid filling the dielectric region of a coaxial line, an electromagnetic wave propagating on the line will both be attenuated and phase shifted as a function of the dielectric constant and conductivity of the fluid. By comparing signals taken from two points on the line a known distance apart, absolute attenuation and phase shift per unit length can be measured. This attenuation and phase shift is then used to calculate the fluid conductivity.

The geometry of a coaxial line measurement is also well suited to continuous measurement in a fluid flow environment. The coaxial line measurement system can be inserted into the fluid flow path without significantly disrupting fluid flow characteristics.

CHAPTER IV

MEASUREMENT SYSTEM ANALYSIS

Introduction

The Response characteristics for the phase shift and attenuation as functions of fluid conductivity and relative permittivity are computed for a TEM mode on a fluid filled coaxial line. The line is assumed to be homogeneous and infinite in length with infinitely conducting wire. Plots at various frequencies are generated. Changes in line characteristic impedance are evaluated and plotted for various frequencies.

Homogeneous Line: Plane-Wave Model

Computations are made using a plane wave analysis to characterize the TEM mode on a coaxial line. To justify the use of a TEM mode plane wave model to describe wave characteristics in a fluid filled coaxial line, the possibility of higher order wave guide modes of propagation were first considered. Given below are equations for the approximate cutoff wavelengths of higher order E and H waveguide modes.[11]

E_{mn} modes

$$\lambda_c = \frac{2\pi(a-b)}{(c-1)\chi_{mn}} \approx \frac{2(a-b)}{n} \quad n = 1, 2, 3 \dots$$

H_{mn} modes

$$\lambda_c = \frac{2\pi(a-b)}{(c-1)\chi'_{mn}} \approx \frac{2(a-b)}{(n-1)} \quad n = 2, 3, 4 \dots$$

Where λ_c is the cutoff wavelength, a is the outer conductor radius, b is the center conductor radius, and c is the ratio of a to b , χ_{mn} is a zero of the Bessel-Neumann function, χ'_{mn} is a zero of the Bessel-Neumann function derivative.

Assuming line parameters of $a = .15$ inches (.00381 meters), $b = .015$ inches (.000381 meters), and $n = 1$, the free space wavelength of the first higher order waveguide mode which propagates is .27 inches (.00686m). This shows that the first higher order mode has a wavelength approximately equal to the outer conductor diameter if the inner conductor is small. For this measurement the minimum operating wavelength will be kept at least several times the outer conductor diameter.

A plane wave analysis was used to predict the wave attenuation and phase shift as a function of fluid conductivity for specific relative permittivities. In the first approximation, finite line axial dimensions are ignored and the conductors are assumed to be infinitely conducting.

Attenuation Response

The attenuation for a TEM mode propagating in an infinite coax filled with a homogeneous lossy media [6] is

$$\alpha = \omega \sqrt{\frac{\mu\epsilon}{2}} \sqrt{\sqrt{1 + \frac{\sigma}{(\omega\epsilon)^2}} - 1} \text{ (NP/m)} \quad \text{EQ. (4)}$$

Where α is the Attenuation, ω is the radian frequency, μ is the magnetic permeability, ϵ is the dielectric permittivity, and σ is the conductivity.

$$\alpha \left(\frac{\text{dB}}{\text{in}} \right) = \alpha \text{ (NP/m)} \times (.2205) \quad \text{EQ. (5)}$$

Equation 5 gives the conversion from Np/m to dB/in. [6] Figure 1 shows the attenuation as a function of fluid conductivity for a range of specific frequencies with a relative permittivity of 80. A relative permittivity of 80 is approximately that of low salinity fluids. Figure 2 illustrates the attenuation range at 100 Mhz as relative permittivity changes from 80 to 2 for low fluid conductivities. As conductivity increases, the range in attenuation as a function of relative permittivity diminishes.

The range over which a change in relative permittivity produces a measurable change in attenuation and phase shift will be used to calculate the percent concentration of

hydrocarbon present in the flowtube. As conductivity increases and the effects of a change in relative permittivity diminish, a prior knowledge of fluid conductivity is required to predict hydrocarbon volume.

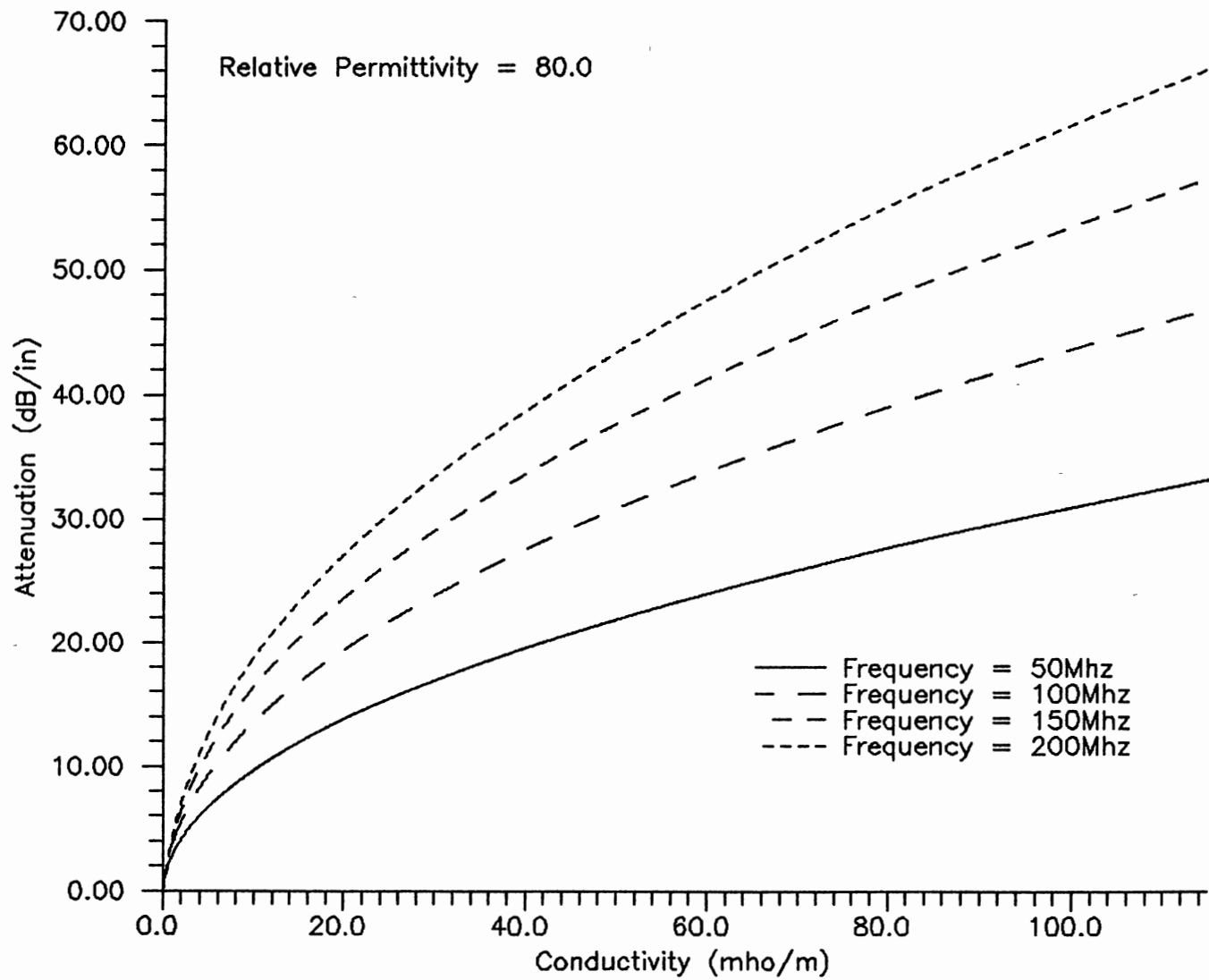


Figure 1. Attenuation Versus Conductivity

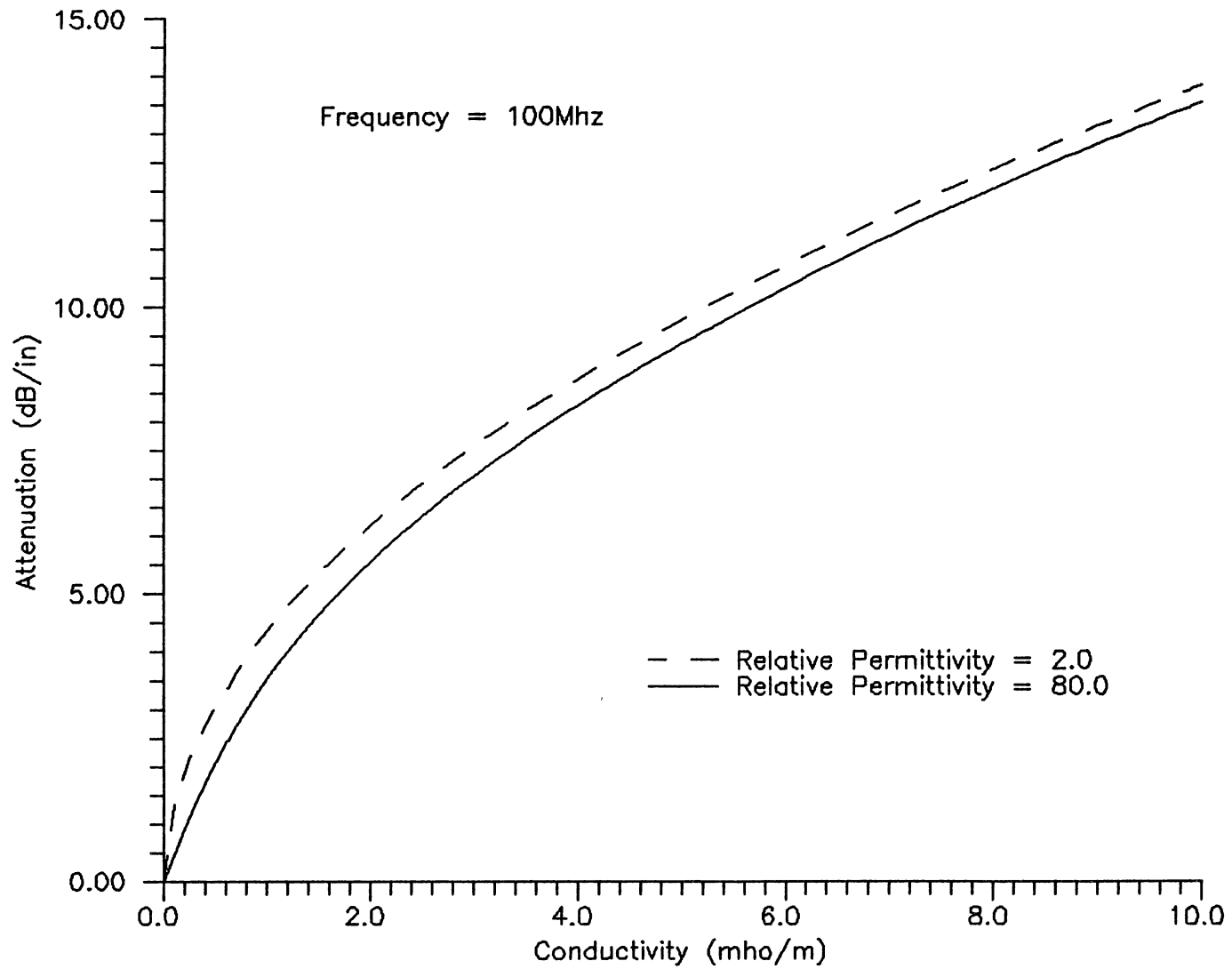


Figure 2. Effects Of Relative Permittivity On Attenuation

Phase Shift Response

The phase shift for a TEM mode propagating in an infinite coax filled with a homogeneous medium is given by [6]

$$\beta = \omega \sqrt{\frac{\mu\epsilon}{2}} \sqrt{\sqrt{1 + \frac{\sigma}{(\omega\epsilon)^2}} + 1} \text{ (RAD/m)} \quad \text{EQ. (6)}$$

where β is the phase shift, ω is the radian frequency, μ is the magnetic permeability, ϵ is the dielectric permittivity, and σ is the conductivity. The phase shift is converted from radians per meter to degrees per inch by

$$\beta \text{ (Degrees/in)} = \beta \text{ (RAD/m)} \times (1.455) \quad \text{EQ. (7)}$$

Figure 3 shows the phase shift as a function of fluid conductivity for a range of specific frequencies with a relative permittivity of 80. Figure 4 illustrates the phase shift spread which can be expected at 100 Mhz as relative permittivity changes from 80 to 2 at low conductivities. As conductivity increases, the effects of changes in relative permittivity diminish.

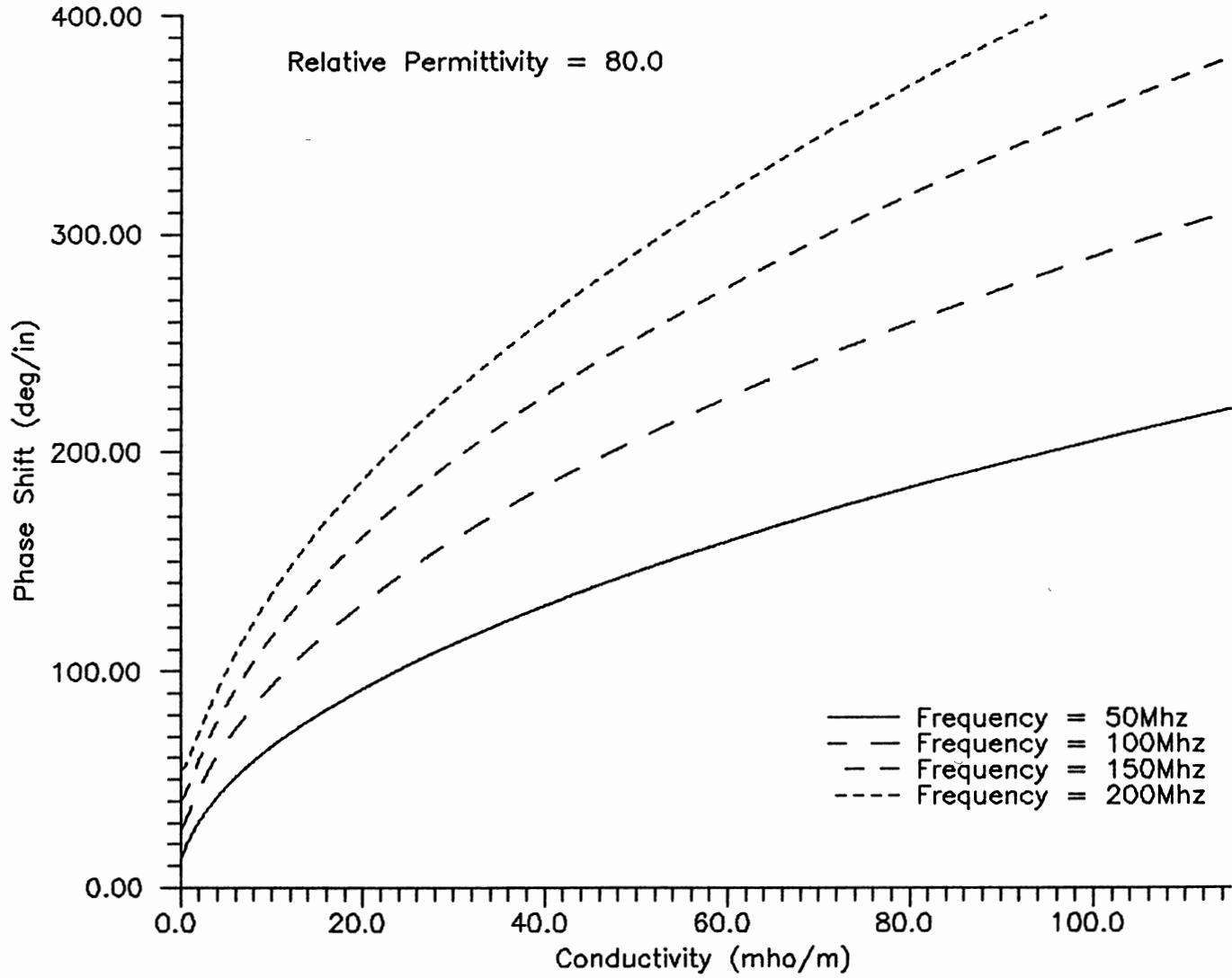


Figure 3. Phase Shift Versus Conductivity

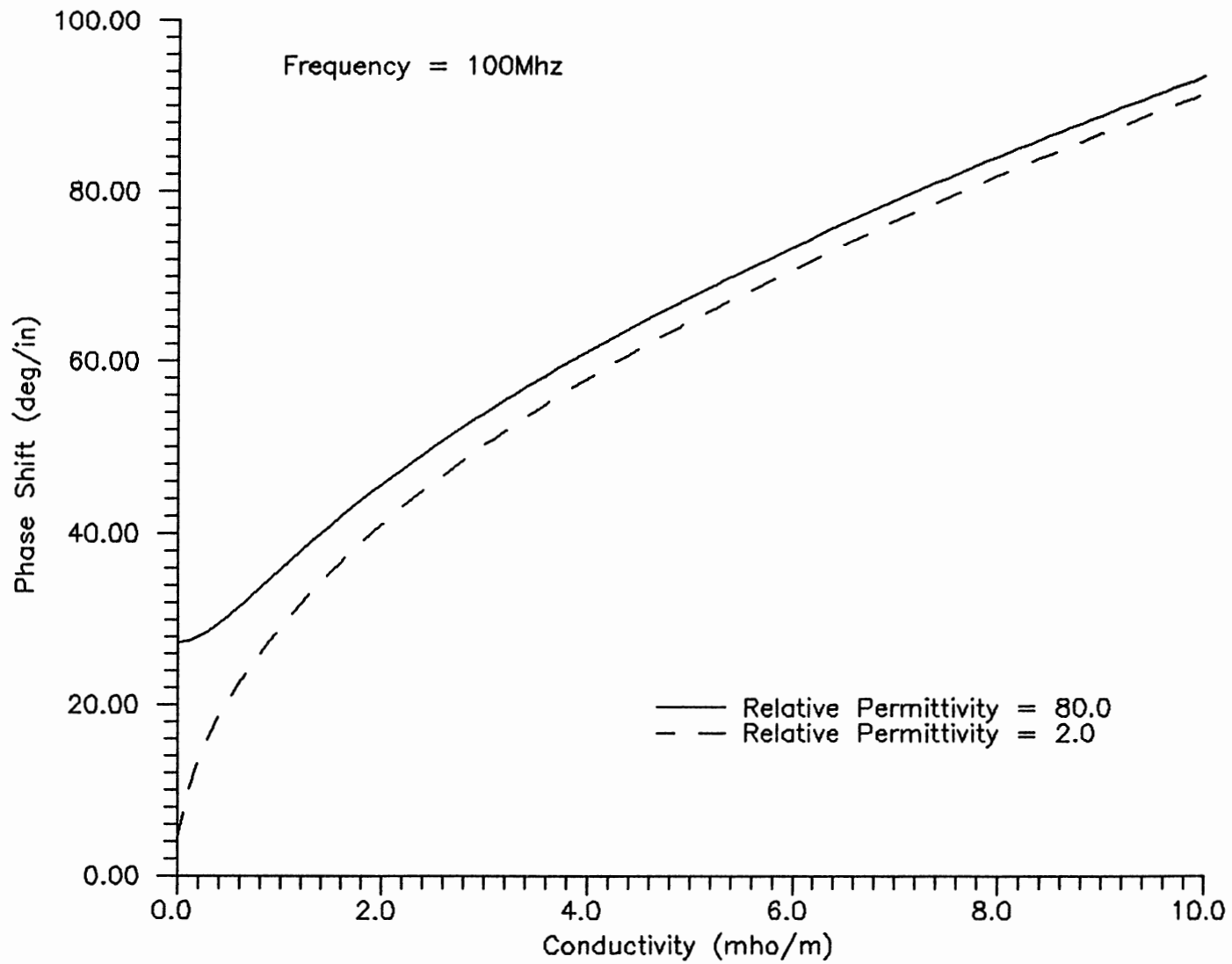


Figure 4. Effects Of Relative Permittivity On Phase Shift

Coaxial Line Characteristic Impedance

The complex characteristic impedance for a lossy coaxial line is [5]

$$Z_c = \sqrt{\mu/\epsilon} \frac{\ln(b/a)}{2\pi} \quad \text{EQ. (7)}$$

$$\text{where } (\epsilon = \epsilon_r \epsilon_0 - j \sigma / \omega) \quad \text{EQ. (7A)}$$

Z_c is the complex characteristic impedance, μ is the magnetic permeability, ϵ_r is the relative dielectric permittivity, ϵ_0 is the free space dielectric permittivity, b is the outer conductor inside diameter, a is the inner conductor outside diameter, σ is the fluid conductivity, and ω is the radian frequency. Figure 5 shows the magnitude of the characteristic impedance as a function of fluid conductivity for specific frequencies with a relative dielectric permittivity of 80. This information is later used in impedance matching the line to the transmitter and receiver electronics.

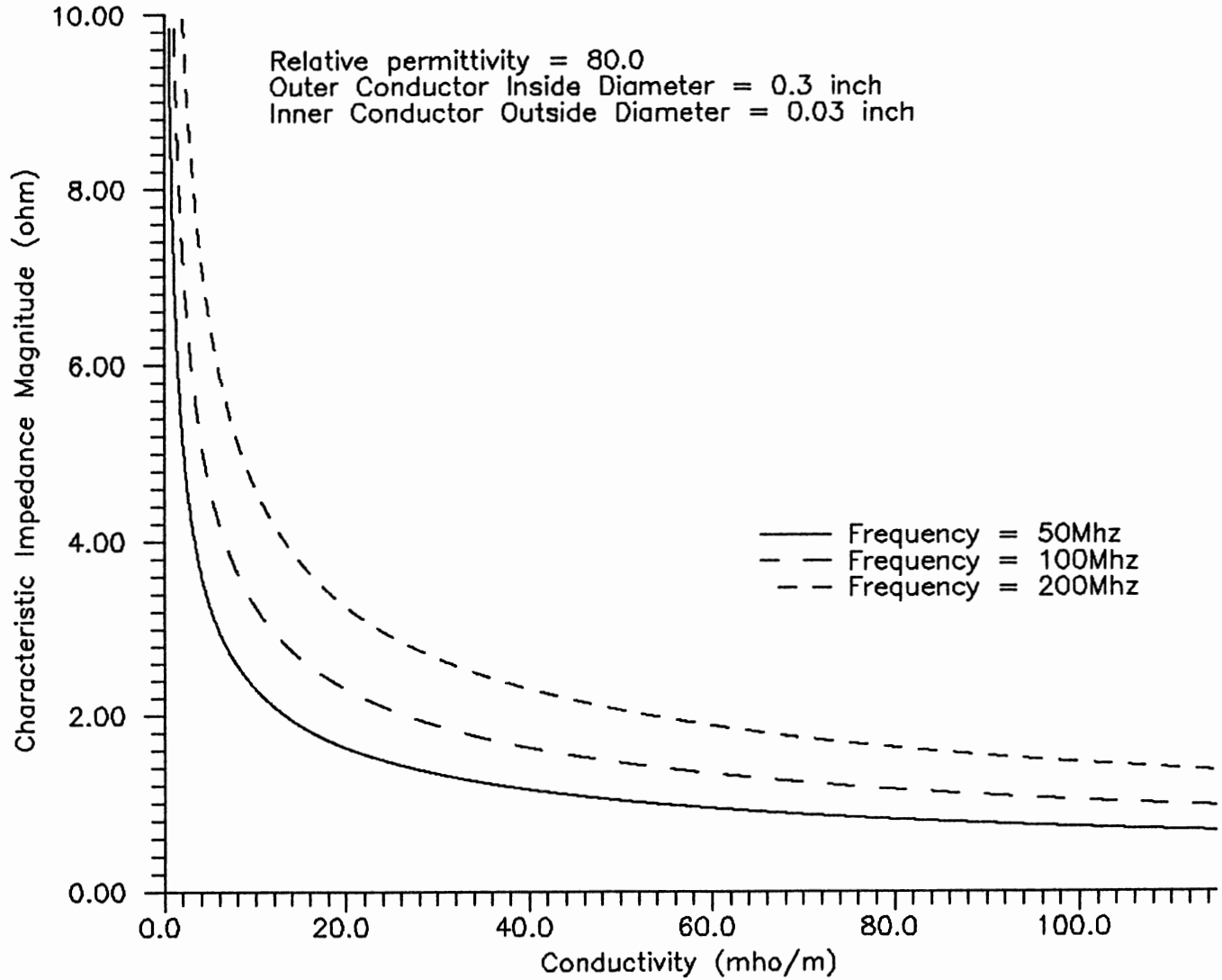


Figure 5. Characteristic Impedance Magnitude Versus Conductivity

CHAPTER V

NETWORK ANALYZER MEASUREMENTS

Introduction

The results of an experimental verification of the TEM mode analysis of characteristic impedance, phase shift, and attenuation of a fluid filled coaxial line are presented in this chapter. The foundation of the measurement system was a Hewlett Packard 4195A Network Analyzer with a 4195ZA Reflection/Transmission test set. A Yellowstone Instruments Model 35 Conductivity Meter with a model 3401 dip probe was used for verification of the fluid conductivity. The phase shift and attenuation were measured as a function of fluid conductivity at several frequencies. The magnitude of the return loss was measured as a function of fluid conductivity and used to compute the magnitude of the characteristic impedance of a fluid filled line.

Characteristic Impedance Set Up

The characteristic impedance of a fluid filled line was measured by determining the magnitude of the reflection coefficient when the fluid filled tube was used as the load of a 50 ohm characteristic impedance measurement set up.[3] The characteristic impedance was then computed by [4]

$$Z_L = Z_c \left(\frac{1 + \Gamma}{1 - \Gamma} \right) \quad \text{EQ. (8)}$$

where Γ is the reflection coefficient, Z_c is the transmission line characteristic impedance, and Z_L is the fluid filled tube characteristic impedance.

As shown in Figure 6, the measurement system consists of the network analyzer fitted with the 50 ohm transmission/reflection test set. The fluid-filled tube is a brass tube that is 6 inches long with an inside diameter of 0.41 inches. The inner conductor has an outside diameter of 0.026 inches and is centered in the tube. One end of the tube is fitted with a coaxial connector and has small holes drilled in the end to prevent trapped air bubbles. The other end of the tube is open. The tube is connected to the 50 ohm test set with a RG58U 50 ohm coaxial cable.

The tube was submersed in a fluid tank and the reflection coefficient was measured. Fluid conductivity was varied and measured using the conductivity meter and probe. Figures 7 and 8 show the measured data plotted with theoretical curves for frequencies of 50 Mhz and 115 Mhz, respectively.

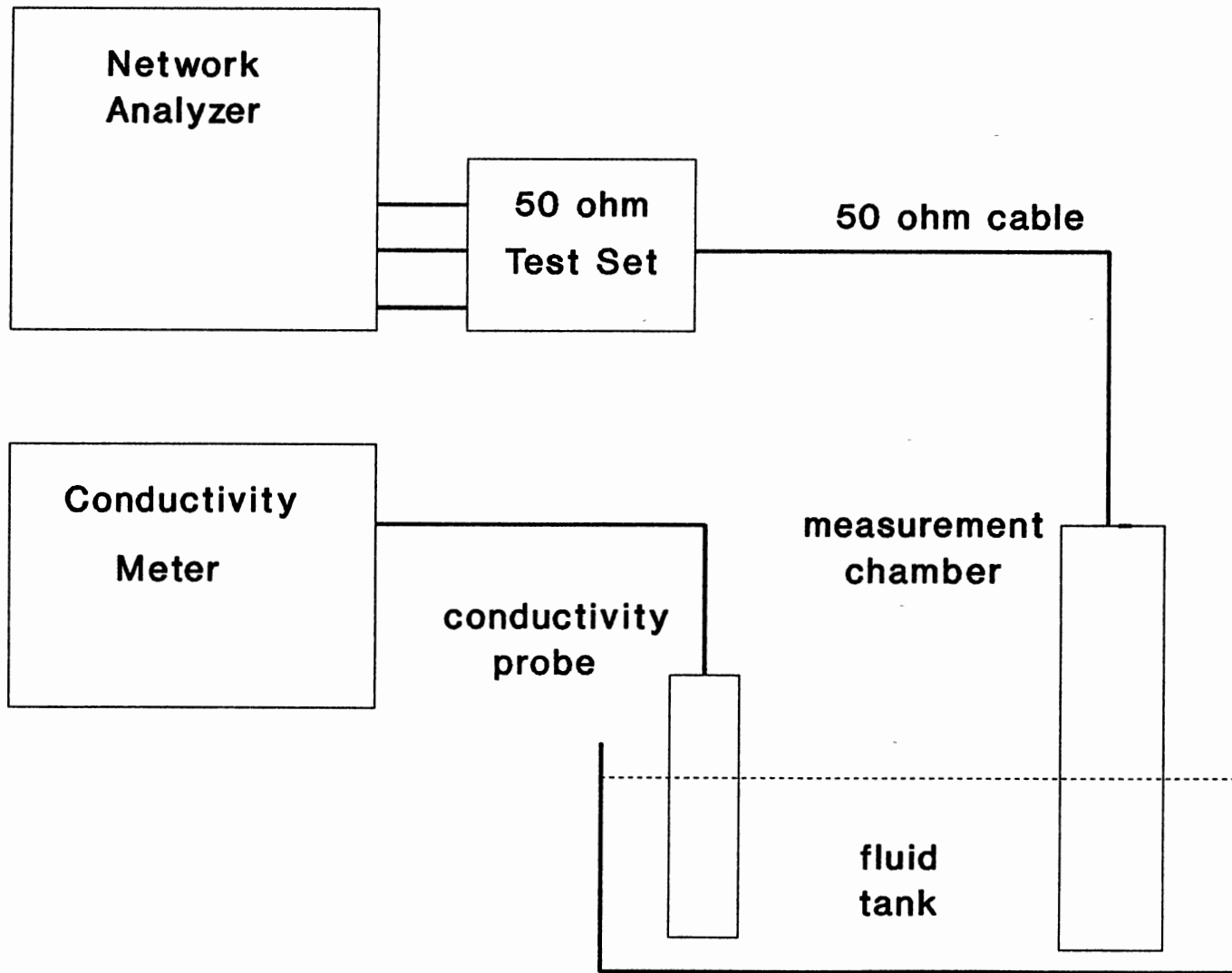


Figure 6. Characteristic Impedance Measurement Setup

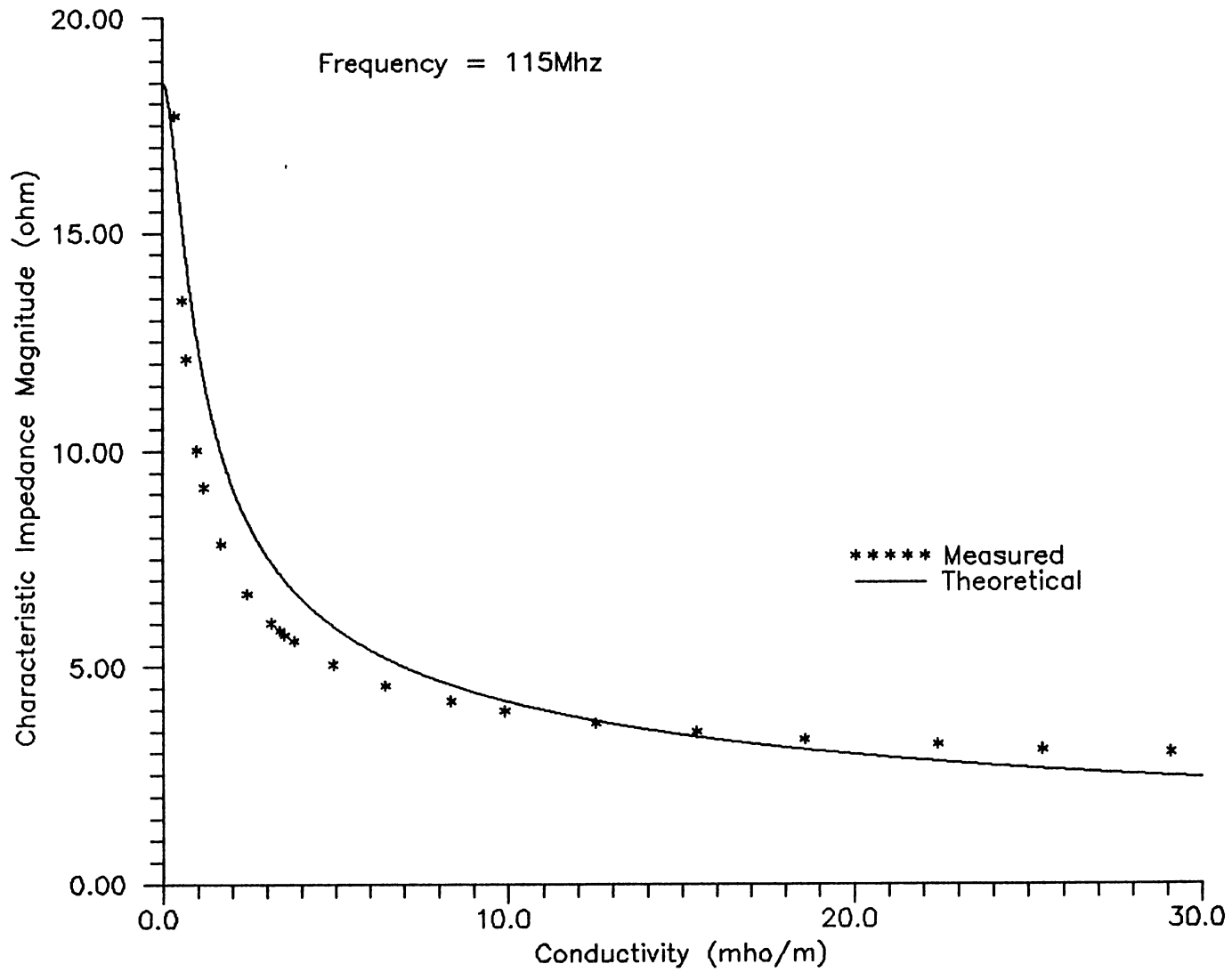


Figure 7. Measured Versus Calculated Characteristic Impedance

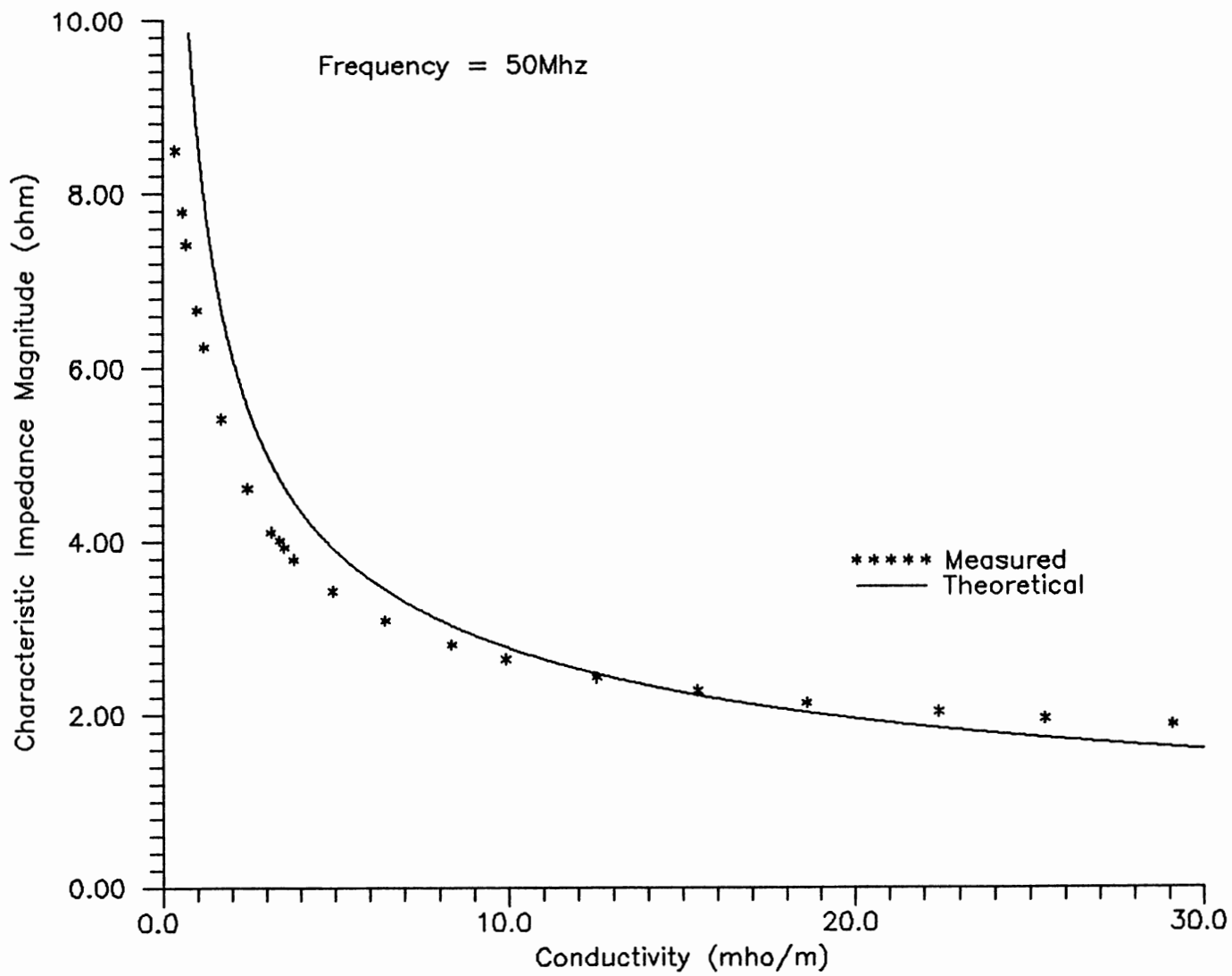


Figure 8. Measured Versus Calculated Characteristic Impedance

Results and Comparison

The analysis only considers the primary reflection and assumes the fluid filled tube to be infinite in length. The comparison between measured and theoretical data in Figures 7 and 8 is good above 10 mhos per meter but only fair below this point, although proper curve character still exists. Attempts to correct the theoretical data using multiple reflections from the open end of the tube show negligible effects on the theoretical curve over the measured data range. Other attempts at correcting theoretical data by varying the reactive component of the reflection coefficient help match theoretical and measured data at specific points but leave the rest of the curve in error.

Slotted Line Set Up

The measurement fixture consists of a brass tube of 3 inches in length that is slotted lengthwise to allow fluid to fill the tube when submersed. Longitudinal slots cut in the outer conductor interfere very little with the signal.[5] The tube is fitted with a center conductor and connected to four 50 ohm coaxial lines as shown in Figure 9. The four connections are spaced by 1 inch. The two cables attached to the center connectors are of equal length and are connected to the network analyzer inputs. One end of the fixture is attached to a cable that is terminated in a 50 ohm matched load to prevent reflections, while the other end is connected to the network analyzer output. In this configuration, the

signal is fed into one end of the tube and coupled out of the tube at the two center ports. With the other end of the tube being terminated, the two output ports are electrically symmetric. The electrical symmetry of the two measurement ports provides equal reflection coefficients for the two ports. Equal reflection coefficients allow the attenuation and phase shift measured between the two ports to be related directly to conductivity without a need to correct for a difference in line mismatch between the two measurement ports. The network analyzer signal was swept from 100 Mhz to 200 Mhz. This configuration allows attenuation and phase shift to be read directly as a function of frequency. The tubes were dipped into a fluid whose conductivity was varied and measured.

Two tubes were constructed and tested. Each had a center conductor outside diameter of 0.03 inches with outer conductor inside diameters of 0.405 inches and 0.285 inches. Figures 10 through 15 show plots of attenuation and phase shift with theoretical curves for frequencies of 100 Mhz, 150 Mhz, and 200 Mhz.

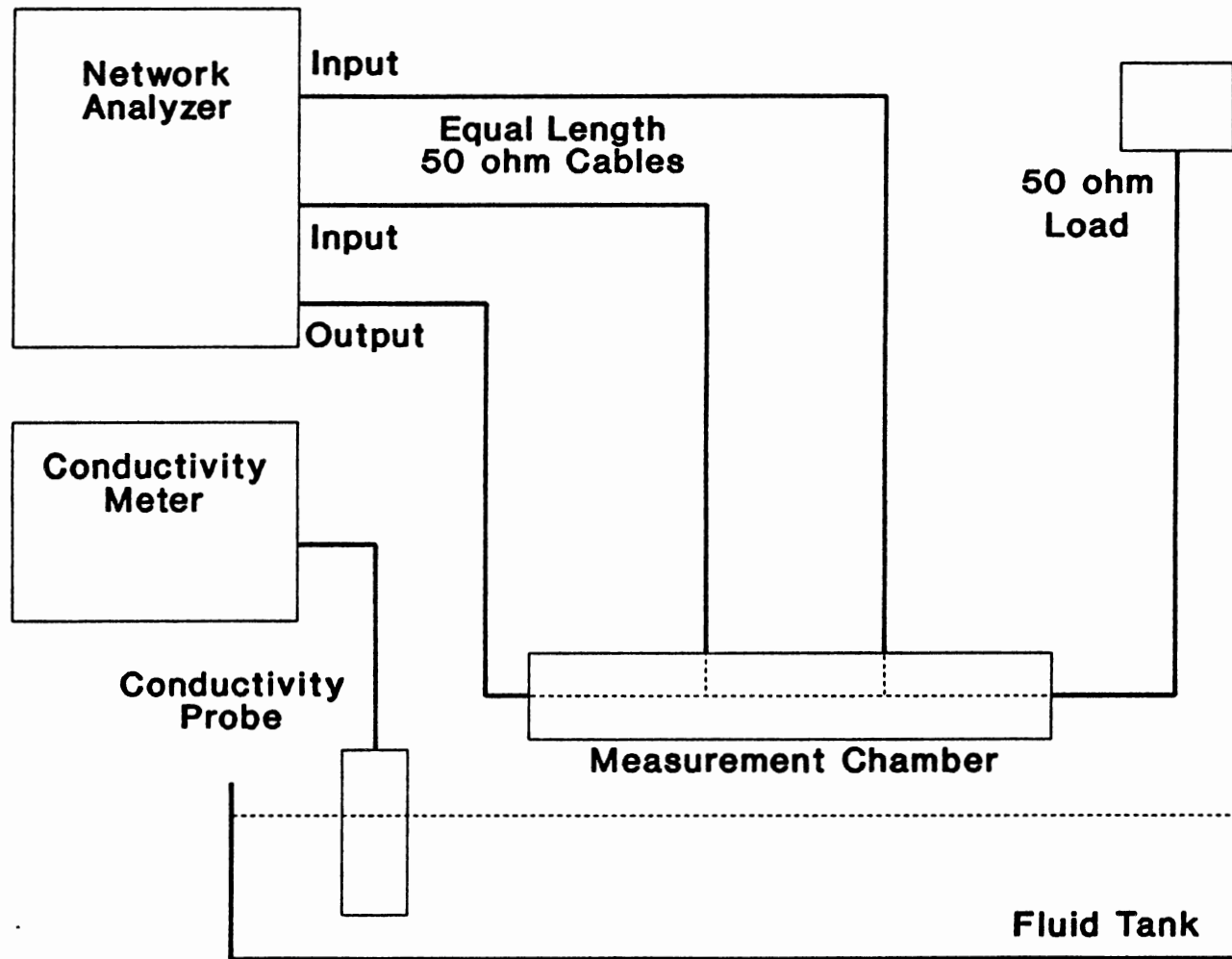


Figure 9. Attenuation Measurement Setup

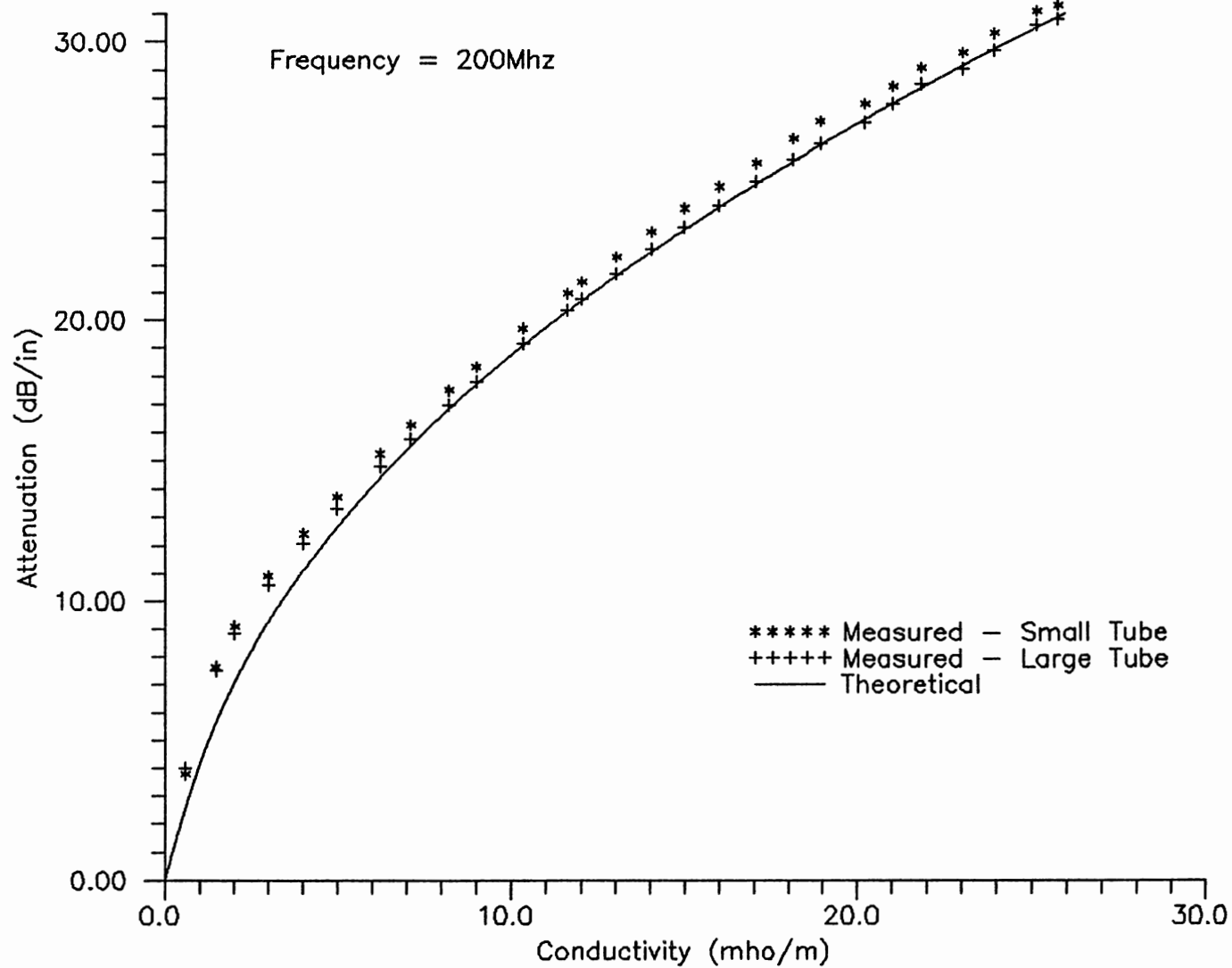


Figure 10. Measured Versus Calculated Attenuation

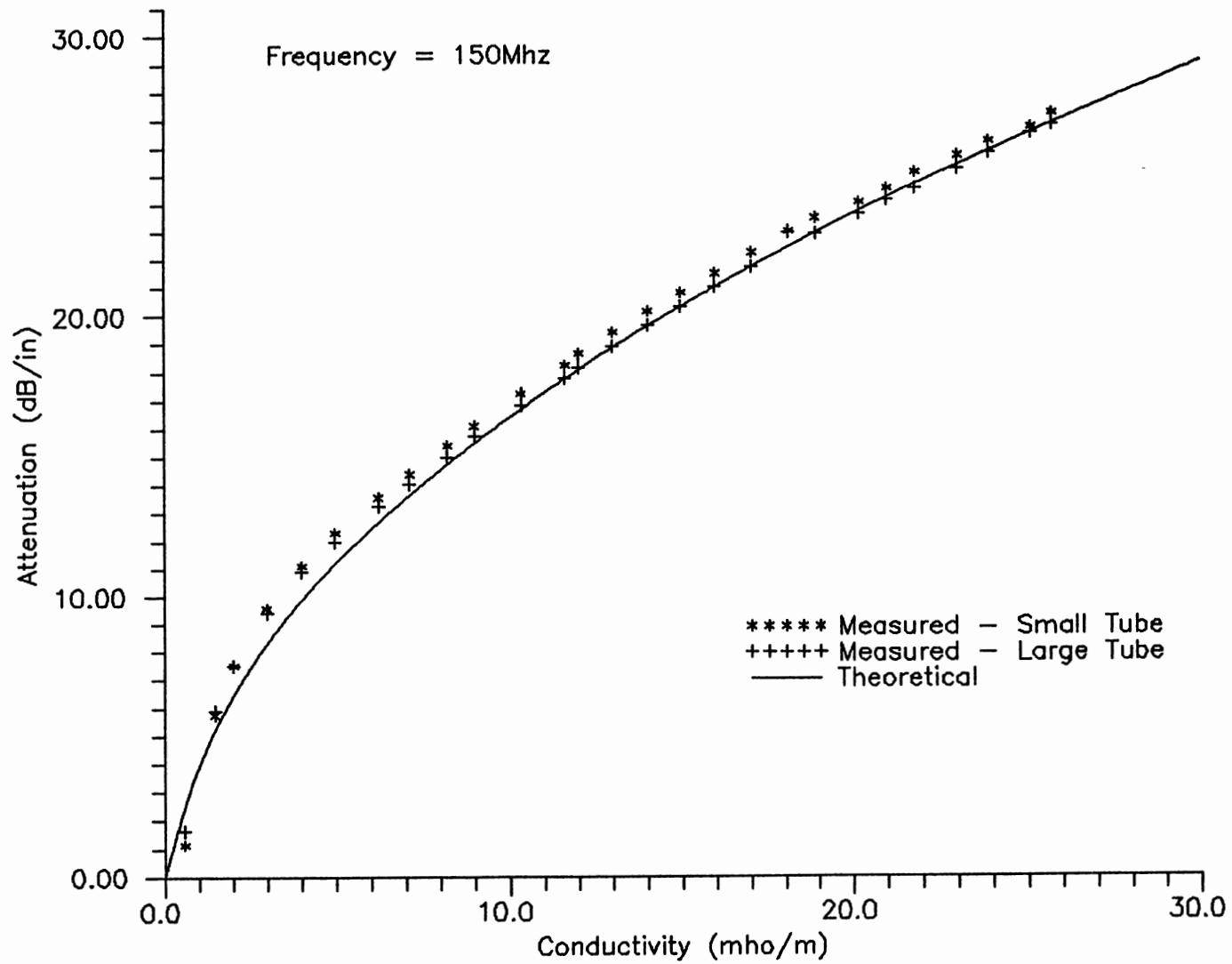


Figure 11. Measured Versus Calculated Attenuation

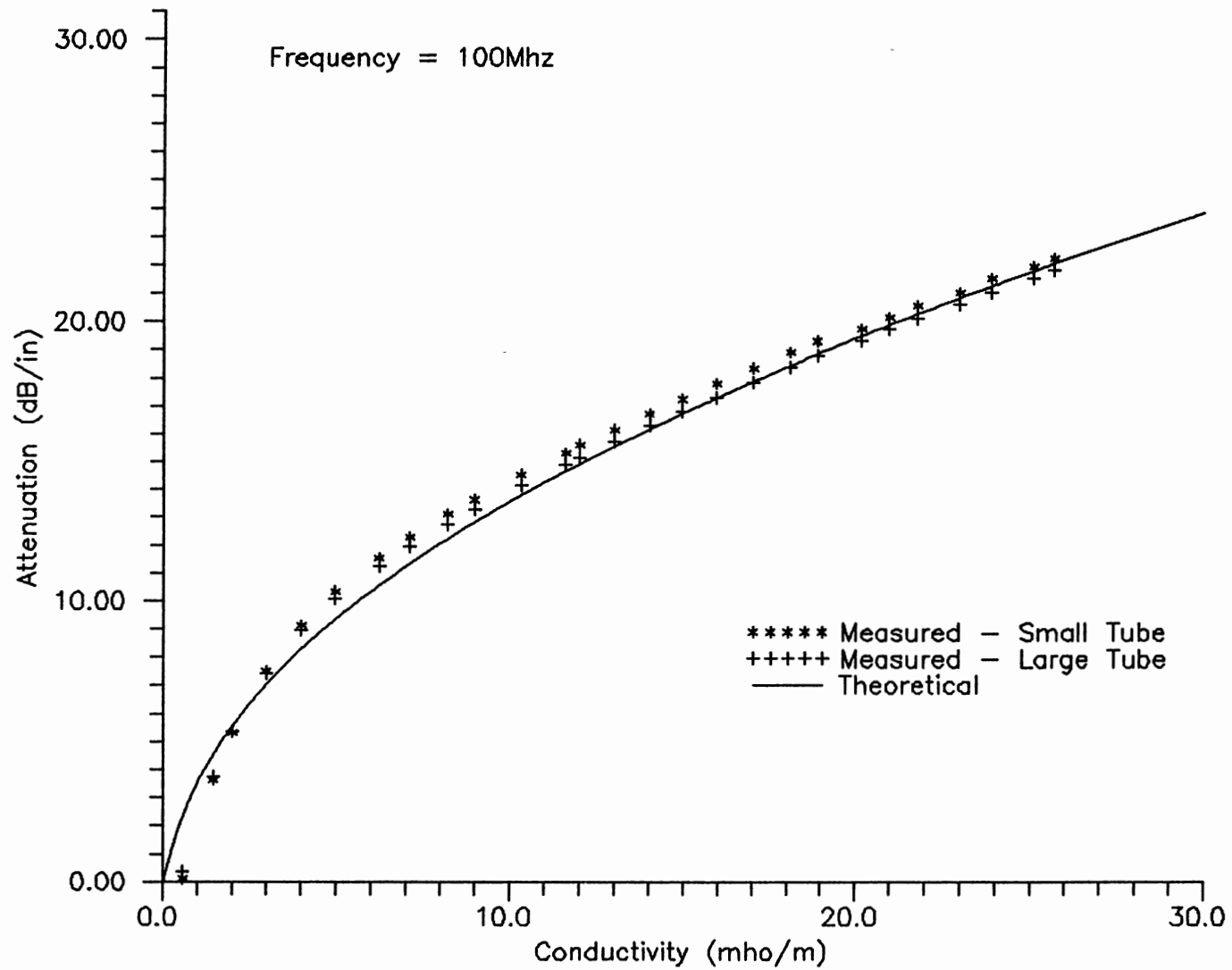


Figure 12. Measured Versus Calculated Attenuation

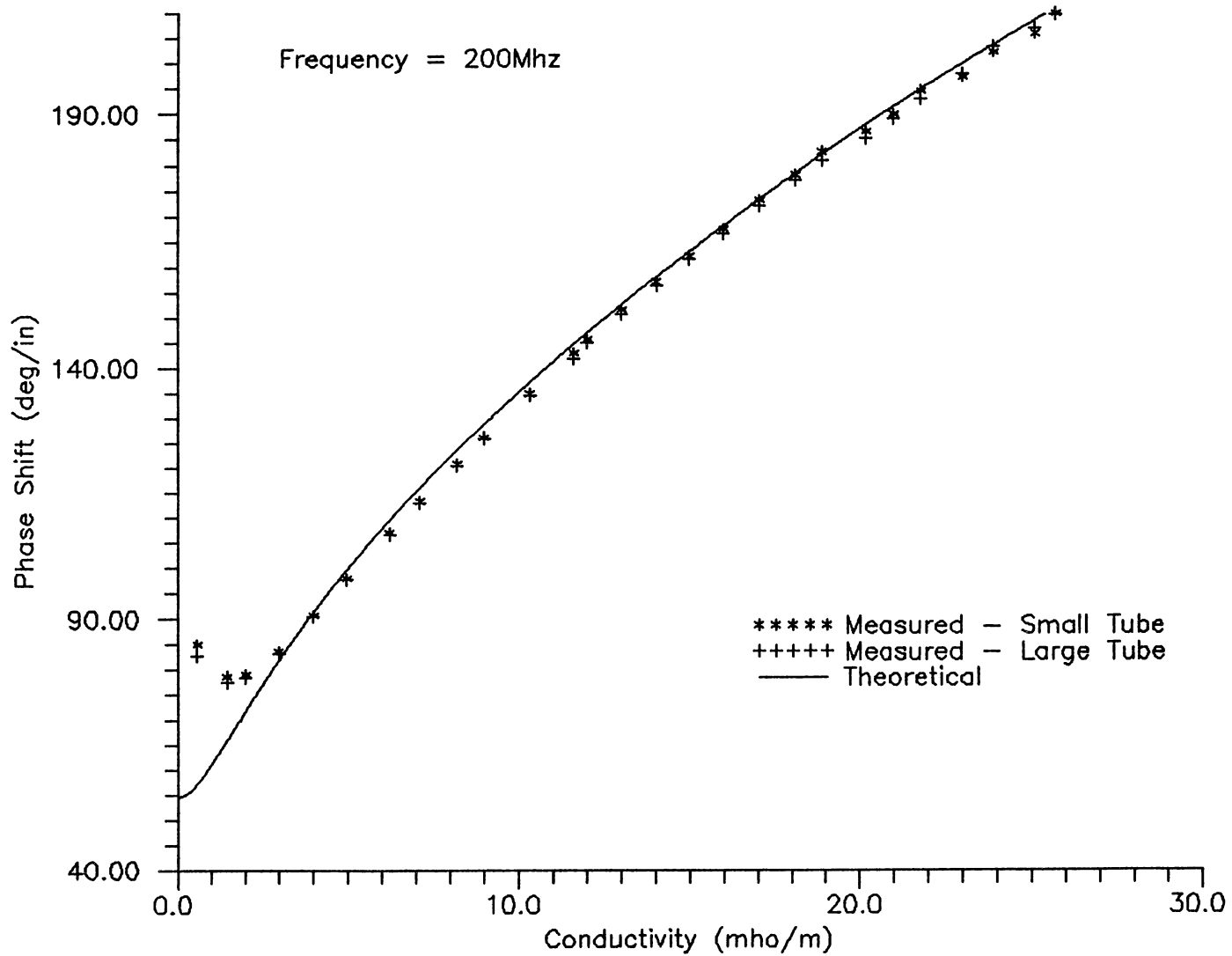


Figure 13. Measured Versus Calculated Phase shift

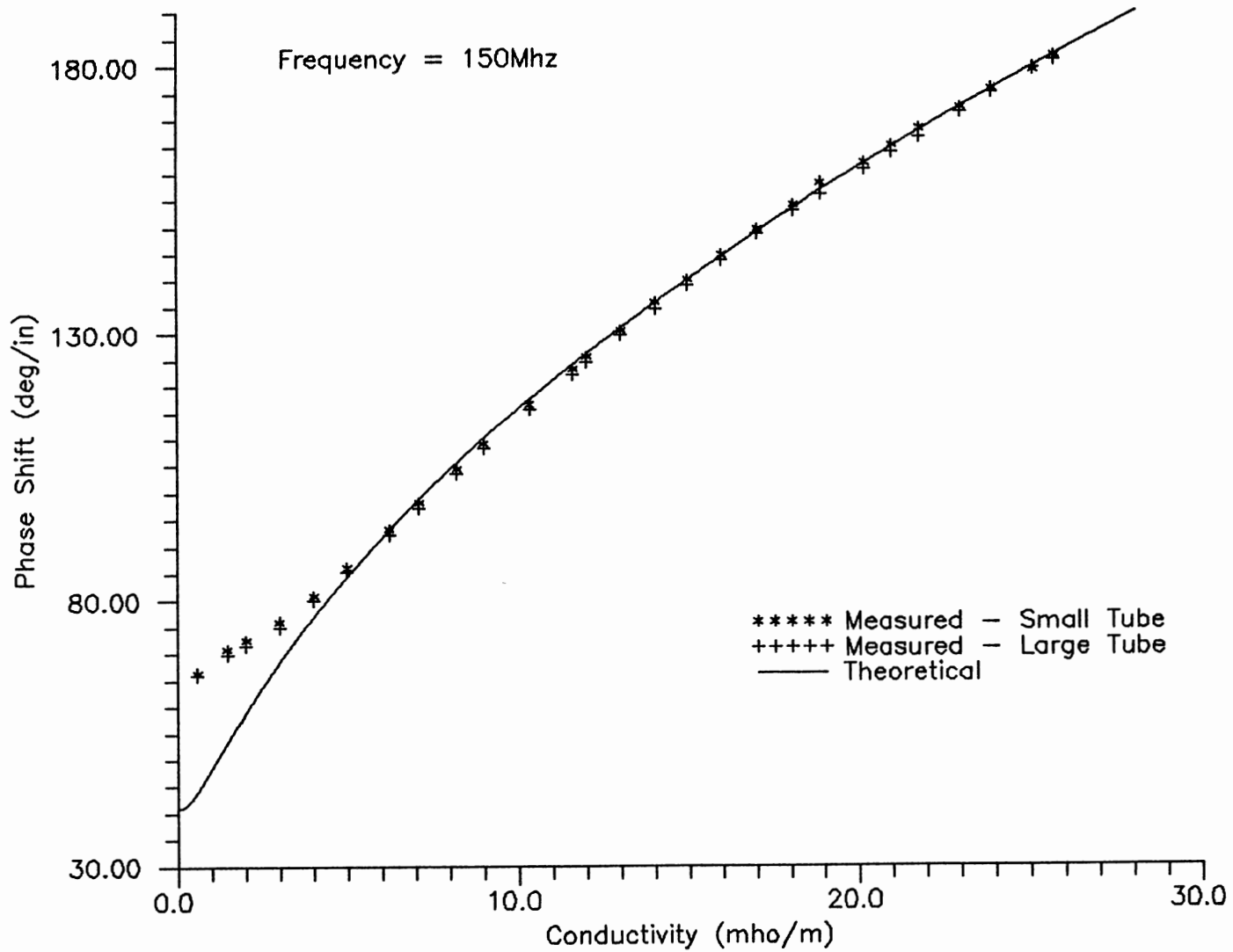


Figure 14. Measured Versus Calculated Phase shift

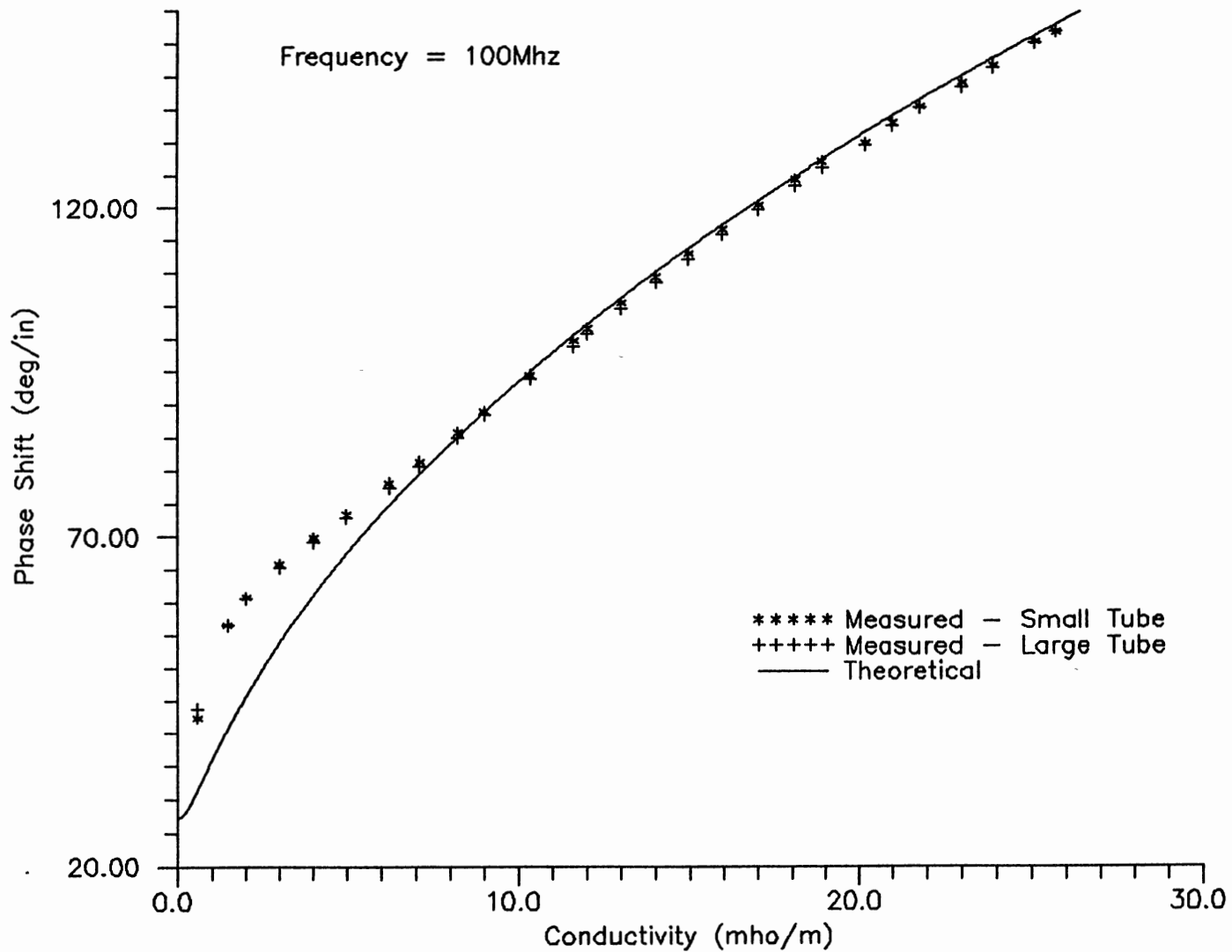


Figure 15. Measured Versus Calculated Phase shift

Results and Comparison

Agreement between measured data and theoretical curves for both phase shift and attenuation is very good for conductivity above 7 mhos per meter. Below this point the measured data begins to deviate somewhat, possibly due to multiple reflections between the measurement ports. Attempts to predict the multiple reflection effects met with little success. This is believed to be due to difficulty in predicting the changing real and imaginary parts of the impedance of the measurement port connections. At the lower conductivities, the attenuation in the tube is not sufficient to damp reflections between ports. The attenuation data shows a small difference between the large and small tube diameters. This is believed to be due to the difficulty in constructing the measurement ports with exactly one inch port spacing. The measured data does show that phase shift and attenuation are essentially independent of tube diameter.

CHAPTER VI

CHOOSING PROTOTYPE SPECIFICATIONS

Introduction

At this point, sufficient analysis and experimental verification has been completed to allow the specification of the geometry and operating frequency of the prototype measurement system. The optimum system will maximize the dependency of the attenuation and the phase shift to changes in fluid conductivity while at the same time keeping electronic complexity to a minimum. Unfortunately, increasing the tube length and/or the operating frequency will increase the measurement sensitivity, but at the expense of increasing electronic complexity (due to increasing signal attenuation). Therefore, a compromise must be made to achieve suitable measurement capabilities. Measurement-tube length and operating frequency will be limited so that reasonable signal levels are maintained over the full operating conductivity range.

Geometry

Design of the measurement-tube geometry has been separated into three categories: tube length, inside and outside conductor diameters, and connector configuration.

The experimental measurements presented earlier show signal deviation from the theoretical planewave response at the lowest conductivities considered. This deviation is due to reflections from line discontinuities that exist at the measurement port connections. At higher conductivity, the increased attenuation damps reflections. Choosing the tube length to be as long as possible will minimize the conductivity at which the deviation becomes significant. Thus, the tube length has been set at three inches, the maximum permitted by the physical specifications of the final product.

The analysis and experimental measurements presented earlier show that the attenuation and phase shift are independent of both the flowtube diameter and the ratio of inside to outside diameter. Line characteristic impedance does vary with the diameter ratio, although for a set diameter ratio characteristic impedance also varies as a function of fluid conductivity. Thus, choosing a diameter ratio for an impedance match would only be valid at a single conductivity. Therefore a 0.3 inch tube was chosen for ease of construction. This is large enough to easily insert and make connection to a center conductor.

The connector configuration was chosen to reduce the effects of reflections due to line discontinuities. All connections to the center conductor are made through the sides of the tube; the ends of the tube are reserved for the attachment of the fluid flow lines. A four-connection

configuration with one inch spacing between all connections was used as shown in Figure 17. A 50 Ohm coaxial line is connected to each of the four ports. One end is used to feed the signal to the center conductor while the 50 Ohm line on the other end is terminated in a matched load. The two center ports are connected to receivers. The one closest to the feed port is referred to as the near receiver, the other is the far receiver. The advantage of this configuration is the impedance symmetry it provides for the receivers. The two receivers see the same impedance looking either direction on the line. This is the same electrical symmetry used when making the network analyzer measurements.

Operating Frequency

To avoid measurement ambiguities, the operating frequency must be kept low enough to avoid a phase shift between the receiver ports in excess of 360 degrees. Previous analysis indicates a phase shift of 360 degrees at the maximum expected conductivity across 1 inch of flow tube at approximately 150 Mhz (see Figure 3). Thus, this is the highest permissible operating frequency for the 1 inch receiver spacings of this test fixture.

The choice of operating frequency as it pertains to attenuation becomes a question of electronic complexity. For higher attenuations, gain compensation must be employed to reduce the range of input signal level over which the phase shift and attenuation measurement circuitry must function.

The range of 30 dB was chosen as the signal level variation after the mixer stages to correspond to the gain range of available gain compensation amplifiers. This represents voltage levels at the detectors from a few hundred millivolts to approximately 10 volts. The gain compensation amplifiers available have an adjustable range of 30 dB. One of these amplifiers will be included in the transmitter and one in the receiver stages. This will allow total system attenuation of 90 dB in the distance from the transmitter to the far receiver (2 inches). From Figure 1, 45 dB per inch attenuation is obtained at an operating frequency of approximately 100 Mhz at the maximum expected conductivity. Using this as the limiting factor, a final system operating frequency of 100 Mhz was chosen.

CHAPTER VII

PROTOTYPE ELECTRONICS CONSTRUCTION

Introduction

An electronic system to implement the measurement system has been designed, constructed, and tested. The system supplies a transmitter signal to the tube and processes the receiver signal to obtain DC voltage signals proportional to signal phase and amplitude differences between the receiver ports.

The prototype electronic system includes a variable gain, 100 Mhz transmitter feeding the fluid flowtube test fixture. The receiver ports of the test fixture are terminated in two identical channels to maintain relative signal amplitude and phase shift. The first stage in each channel is a variable gain amplifier which feeds a frequency mixer. The mixer is driven by a 99.980 Mhz local oscillator, producing (when mixed with the 100 Mhz test signal) a 20 khz intermediate frequency (IF) signal. The intermediate frequency amplifier filters out the unwanted mixer side bands and amplifies the desired signals before passing them on to the phase and amplitude detection circuitry. The amplitude detector output then supplies a control voltage which is fed to the variable gain amplifiers to control total system gain.

Controlling system gain allows the use of phase and amplitude detectors with dynamic ranges of only a fraction of the total system dynamic range. This makes the measurement accuracy over the full system range much easier to achieve.

The electronic techniques utilized in the design and construction of the intermediate frequency amplifier, phase detector, and amplitude detector were derived from existing circuitry that has been observed to function at temperatures in excess of 350°F. (Although the components used in the prototype are standard shelf items, many of which will not withstand elevated temperatures.) With little more than a component upgrade these circuits should function over the required temperature range.

Flowtube

The flowtube assembly is shown in Figure 17. The flowtube measurement chamber is constructed of brass tube with an inside diameter of 0.31 inches. Four holes were drilled along a line on the side of the tube spaced by one inch. The tube wall, 180 degrees adjacent to these holes, was removed to allow soldering a center conductor in place. The center conductor is a copper tube with an outside diameter of 0.09 inches. The center conductor also has 4 holes drilled 1 inch apart to accommodate a feed-thru connector. The feed-thru connector has a center conductor and a threaded outer shield fitted with an outer o-ring seal, with a glass seal between the center and outer conductor.

Brass fixtures were milled to fit the flowtube outside radius. Threads to mate with the feed thru connector and an o-ring seat were also machined. Assembly of the flowtube measurement chamber was accomplished by installing the feed-thru connectors into the brass fixtures and positioning them over the 4 flowtube holes. The fixtures were then soldered to the flowtube. The flowtube center conductor was then positioned over the feed thru connectors and soldered in place through the back side of the flowtube. The back side of the flowtube was then soldered back in place. The assembled flowtube is shown immersed in a test fluid in Figure 25.

Transmitter

The transmitter supplies a variable amplitude, 100 Mhz signal to the test fixture input. The signal amplitude is controlled by feedback from the amplitude detector section.

The circuit oscillator is a Champion Technologies K1149CA ECL Crystal Clock Oscillator, which supplies 0 db at 100 Mhz. The oscillator output is fed to a Hewlett-Packard Hamp 4001 Variable Gain Amplifier. The Hamp 4001 is gain controllable from approximately -10 dB to 20 dB. Following the variable gain amplifier are two common emitter configuration gain stages, each with approximately 10 dB of gain. Each stage includes an NTE473 PNP Transistor. Efforts to electrically match these stages to the measurement chamber proved fruitless due to the large variation in the

characteristic impedance of the chamber with changing fluid salinity. The ratio of the signal generated to the signal coupled into the tube varies due to the mismatch, but this is compensated by the automatic gain compensation circuitry.

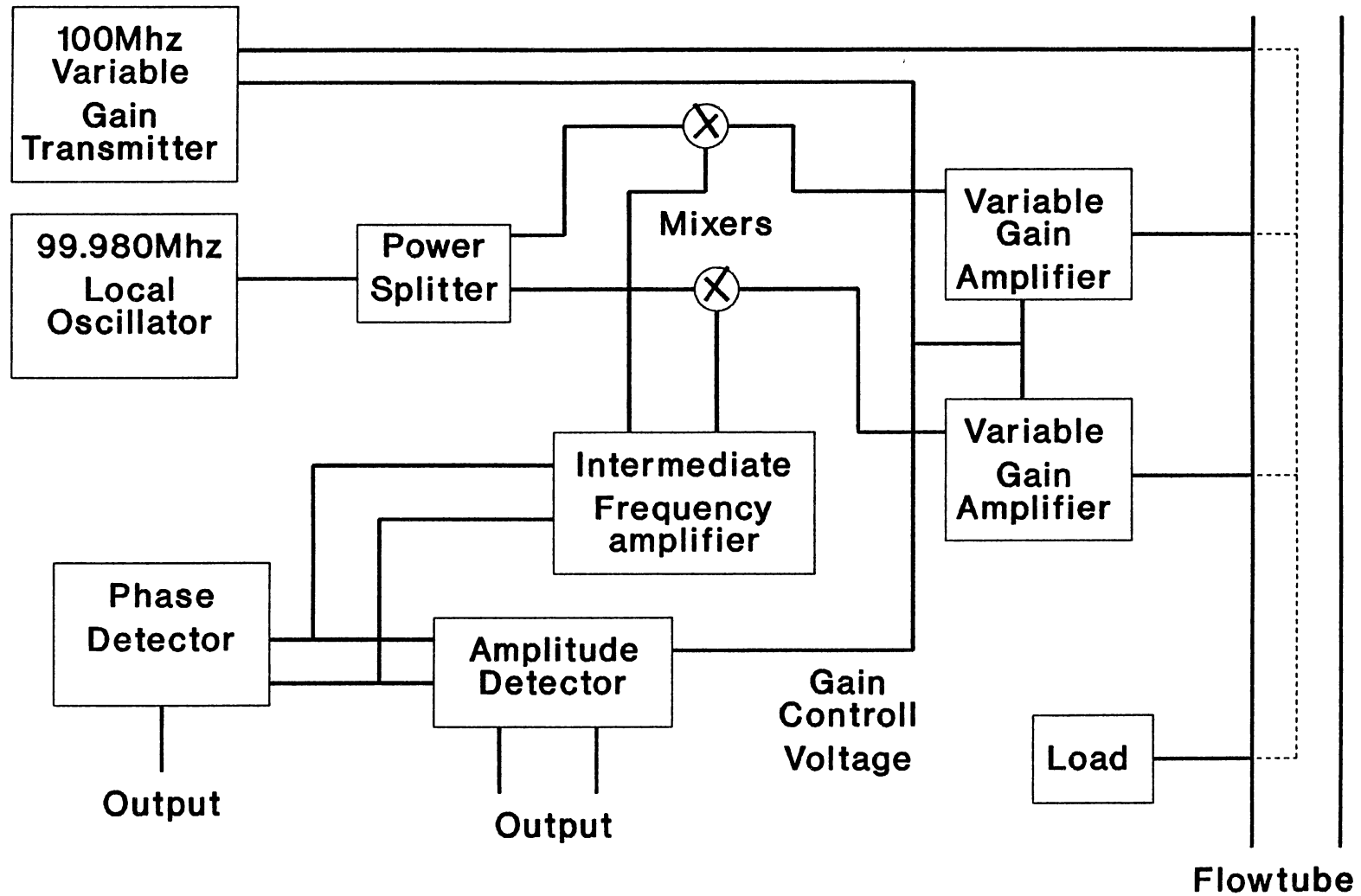


Figure 16. Measurement System Block Diagram

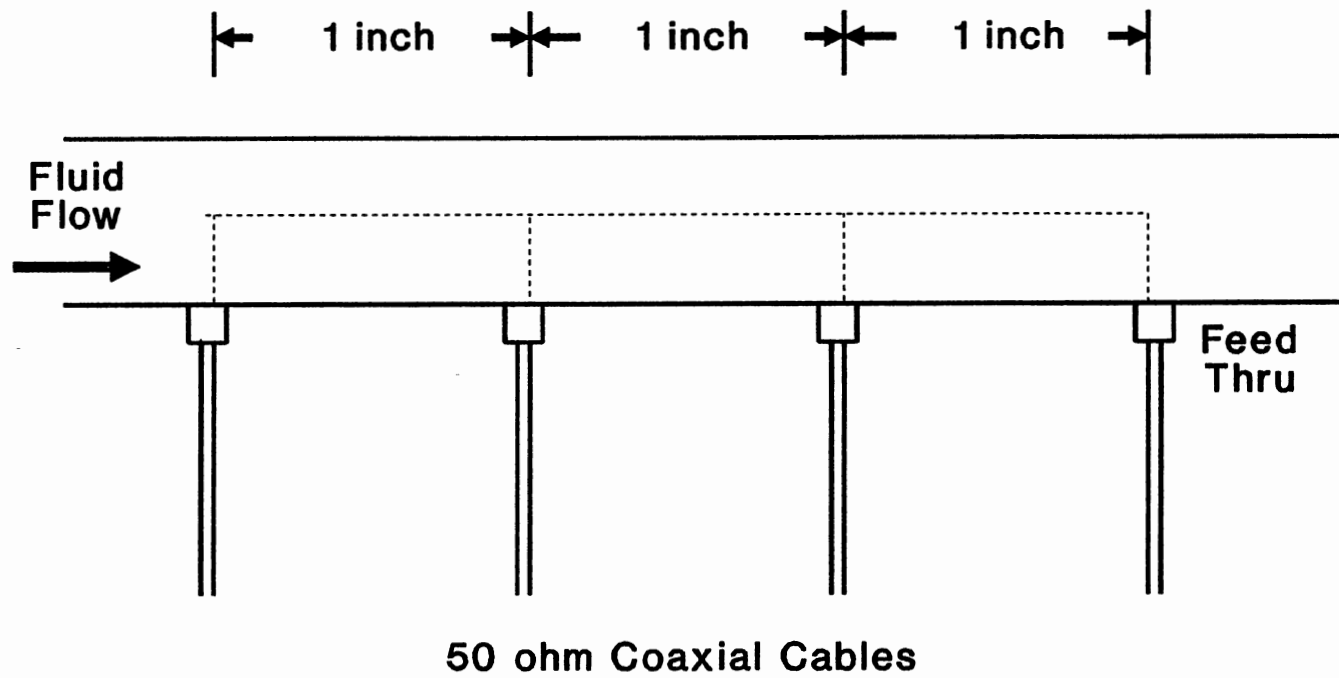


Figure 17. Flowtube Measurement Chamber

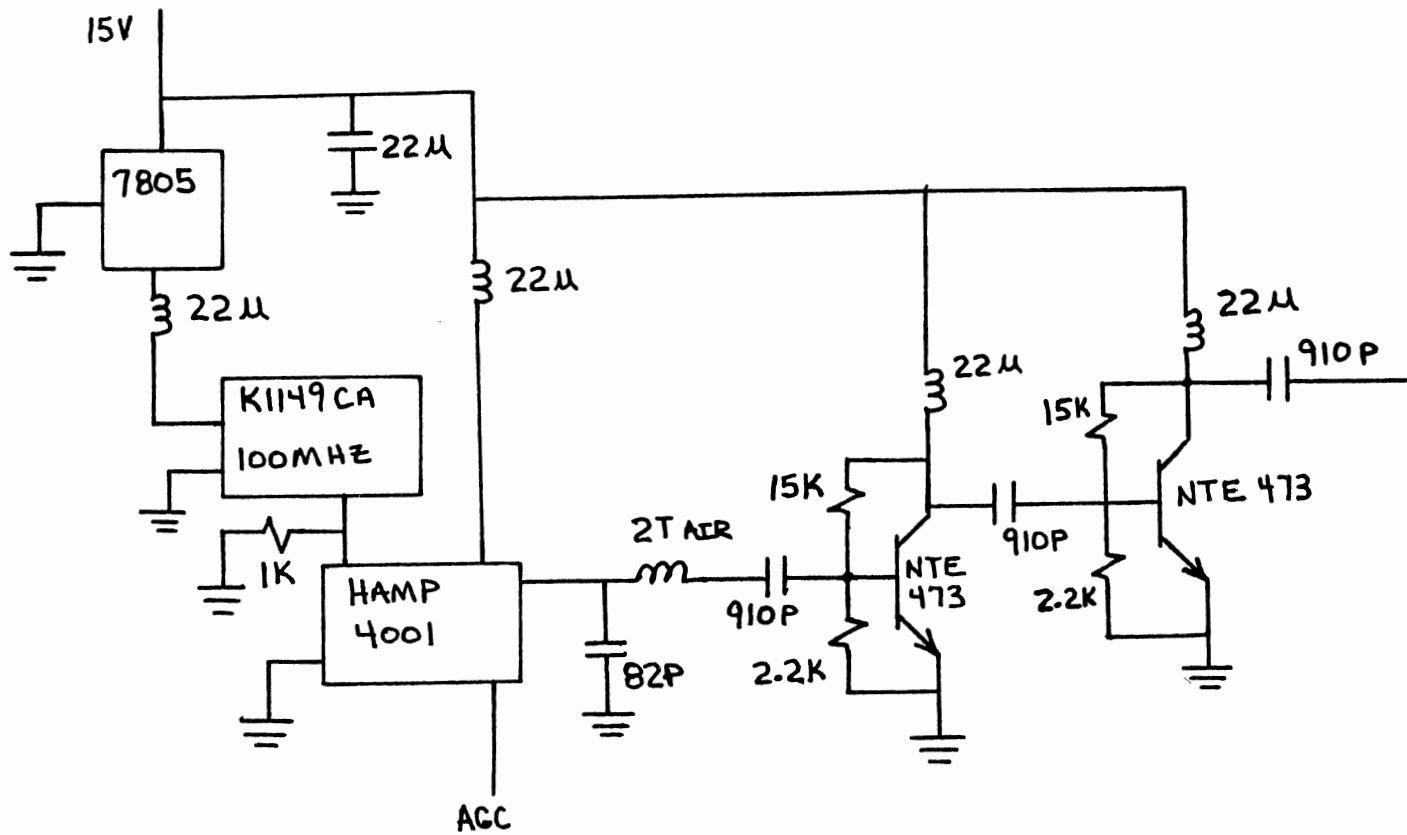


Figure 18. Transmitter Schematic

Local Oscillator

The local oscillator, shown in Figure 19, supplies two constant level, equal phase 99.98 Mhz signals to the mixer for frequency shifting of the received signal.

The circuit oscillator is a Sentry Manufacturing Series Resonant 99.980 Mhz Crystal. The crystal and a Hewlett Packard HXTR 5101 Transistor are set up in a Colpitts Oscillator configuration, [2]. The oscillator output is amplified by a Hewlett Packard HMPA 0335 Monolithic Amplifier. In the final stage, the oscillator power is divided by a Mini-Circuits PSC2-1 two-way, zero phase power splitter. The final output consists of two equal phase 99.980 Mhz signals at approximately 7 dB.

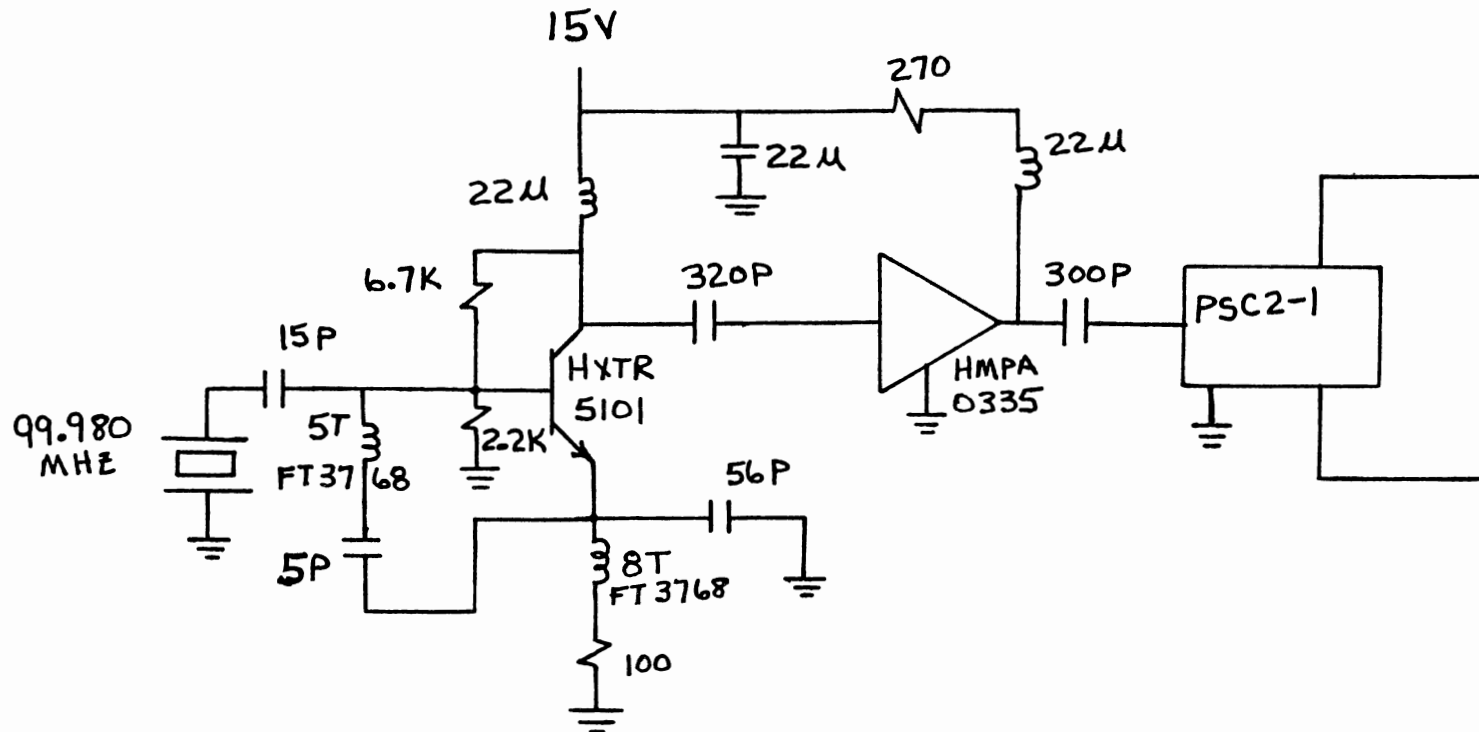


Figure 19. Local Oscillator Schematic

Mixer

The mixer circuit is shown in Figure 20. It consists of two identical channels which convert the two received 100 Mhz measurement chamber signals into two 20 khz intermediate frequency signals while preserving their relative amplitude and phase difference. There are 5 inputs and two outputs on this board. The first two inputs are 99.980 Mhz signals from the local oscillator. These two signals are fed to a pair of amplifier gain stages. The first is a Hewlett Packard HPMA 0335 Monolithic Amplifier and the second is a NTE346 in a common emitter configuration. These gain stages are needed to amplify the local oscillator signals to 23 dB to drive the two Mini-Circuits SAY-1 frequency mixers. Two additional inputs are the 100 Mhz signals from the measurement chamber. They feed the Hewlett Packard HAMP 4001 Variable gain amplifiers that comprise the second stage of gain control. The fifth input is the gain control voltage from the amplitude detector. The outputs from the frequency mixers are coupled to an intermediate frequency amplifier and filter board. The SRA-1mH mixer shown in Figure 20 was the only available replacement after one of the SAY-1 mixers failed. The difference in phase shift between the two mixers is compensated on the intermediate frequency amplifier.

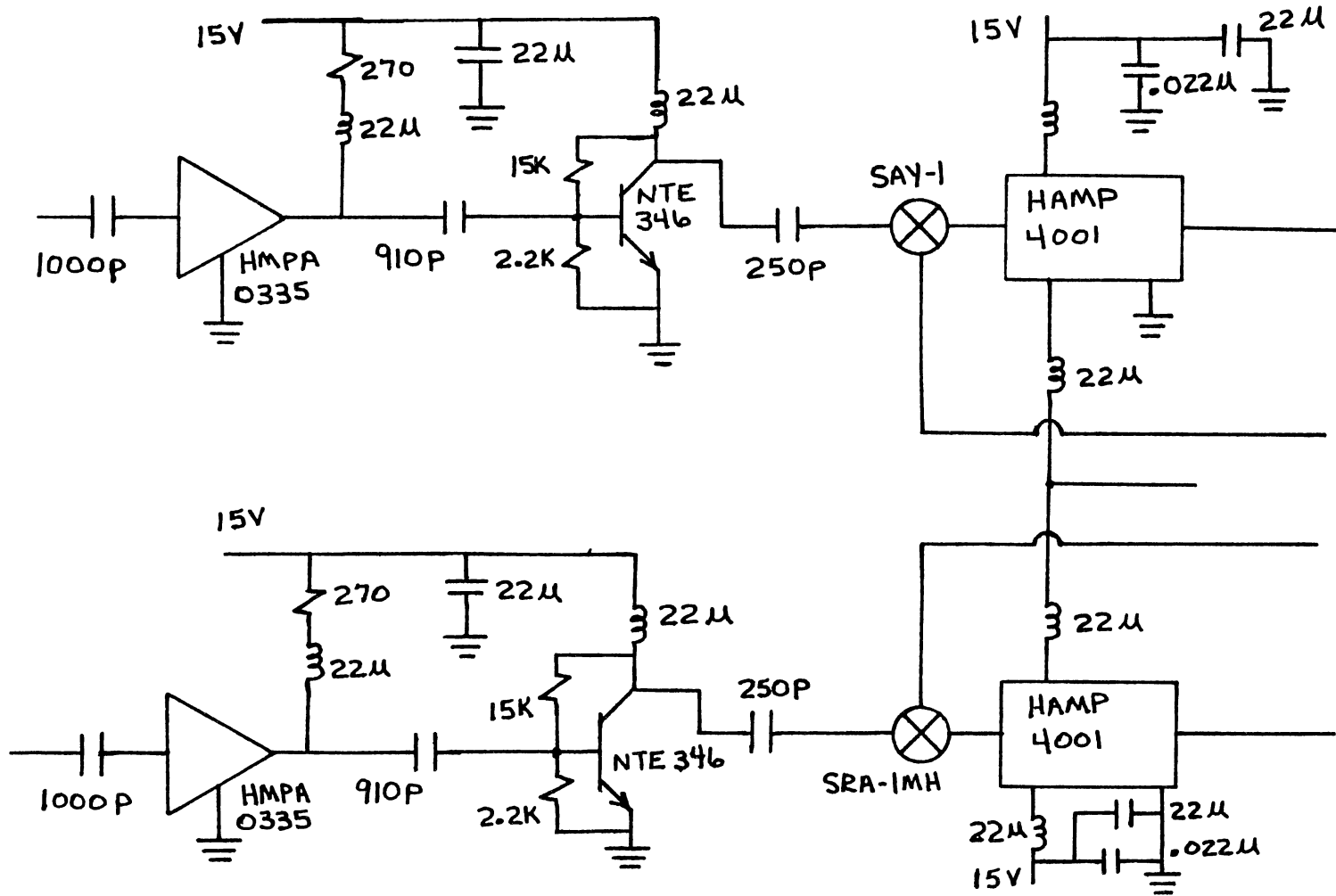


Figure 20. Mixer Schematic

Intermediate Frequency Amp

The intermediate frequency amplifier shown in Figure 21 filters any unwanted mixer sidebands, amplifies the signal, and outputs it to the detector circuitry.

The intermediate frequency amplifier consists of two identical channels, each with 3 inverting amplifier stages of 20 dB gain. The amplifier stages are coupled by single pole lowpass filters whose break frequencies are approximately 28 khz. The two channels are identical to maintain relative amplitude and phase shift between the two receiver signals. One channel includes an extra unity gain inverting amplifier. This stage was necessary to compensate for a 180 degree phase shift introduced by the replacement SRA-1MH mixer after the failure of one of the SAY-1 mixers in the original matched pair, as described in the previous section.

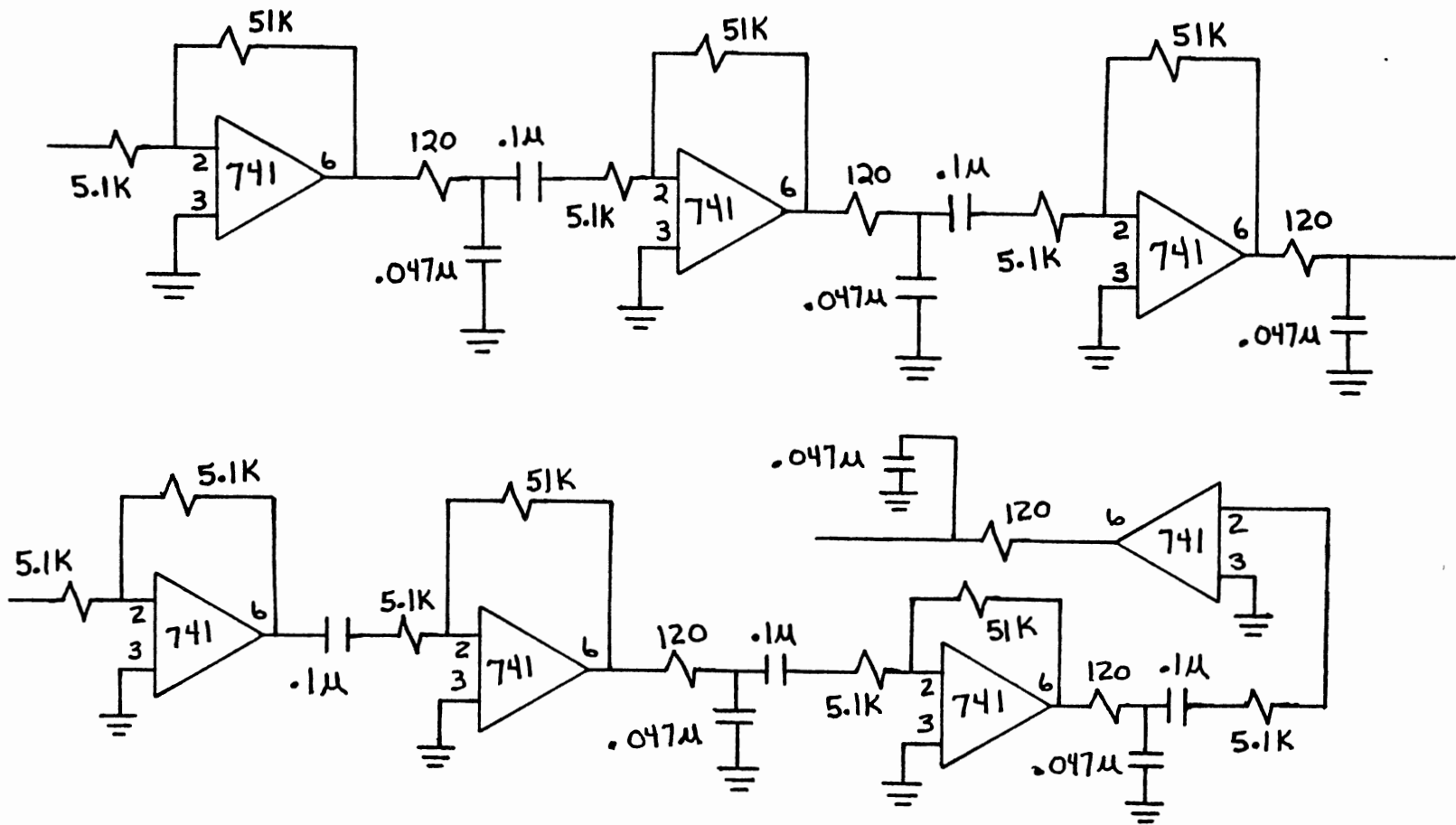


Figure 21. Intermediate Frequency Amplifier Schematic

Phase Detector

The phase detector, shown in Figure 22, generates a DC level proportional to the phase difference between the two receiver channels.

The two 20 khz receiver signals from the intermediate frequency amplifier are input to the phase detector. The first amplifier stage is a high gain inverting amplifier which is diode clipped at 1.4V at the output to give a first approximation to a square wave. This output is then fed to a comparator to produce a true square wave output. The amplifier and comparator are identical in each channel so the two square waves maintain relative phase. The two square waves are applied to the clock pins of two D flip-flops, with D lines tied high and the Q lines tied to the reset. This gives an output pulse on the input rising edge transitions that is approximately 20 ns wide. The spacing between these pulses is proportional to the phase shift between the input signals. The pulses are then sent to another D flip-flop with the near receiver channel tied to clock and the far receiver channel tied to reset. The result is a pulse train that is integrated to yield a DC level proportional to the phase difference between the two receiver signals with a final amplifier stage to adjust DC output sensitivity.

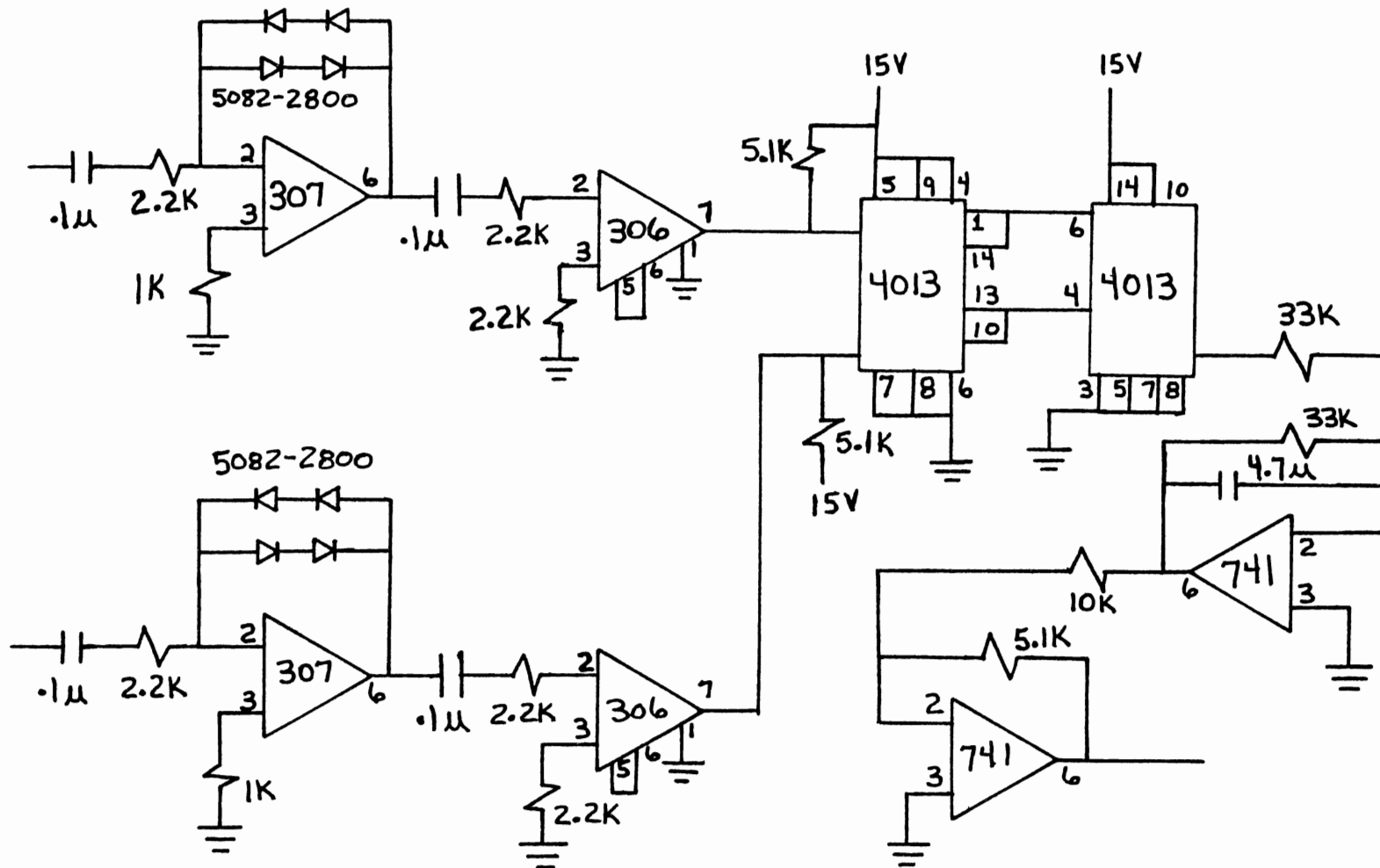


Figure 22. Phase Detector Schematic

Amplitude Detectors

The amplitude detectors shown in Figure 23 are full wave rectifiers followed by integrators to produce DC levels proportional to the RMS value of the input sine waves.

The amplitude detector inputs are two 20 khz receiver signals from the intermediate frequency amplifier. The circuit consists of two identical channels. First is a two-stage full-wave rectifier followed by an integrator to obtain the two DC level outputs, all realized using 741 operational amplifier.

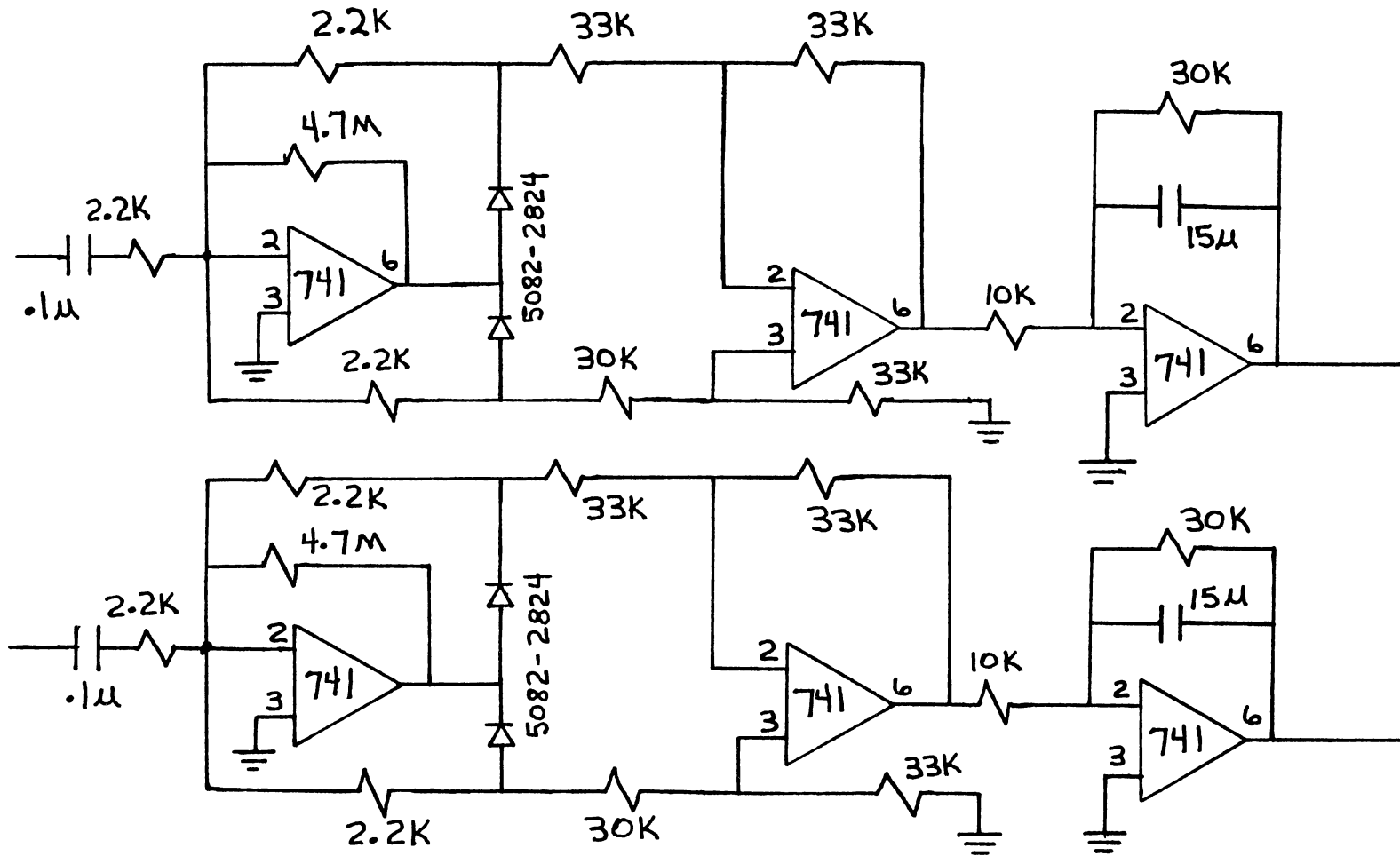


Figure 23. Amplitude Detector Schematic

Automatic Gain Control

As shown in Figure 24, a control voltage is developed for automatic receiver/transmitter gain adjustment by monitoring the output of the amplitude detector of the near receiver channel. The circuit consists of an inverting amplifier feeding a comparator. The comparator output is low-pass filtered and amplified by a noninverting amplifier for increased current drive.

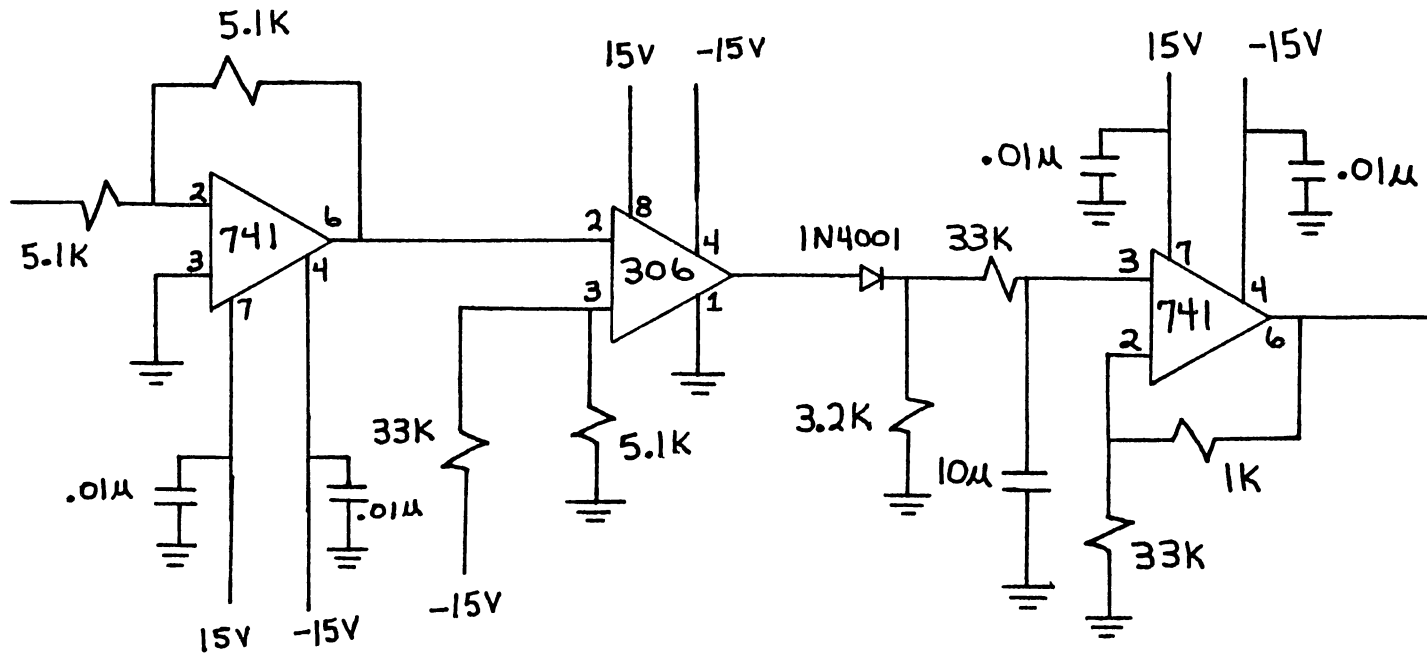


Figure 24. Automatic Gain Compensation Schematic

Assembled System

Figure 25 is a photograph of the assembled measurement system. Figure 26 shows the layout of the individual components of the system.

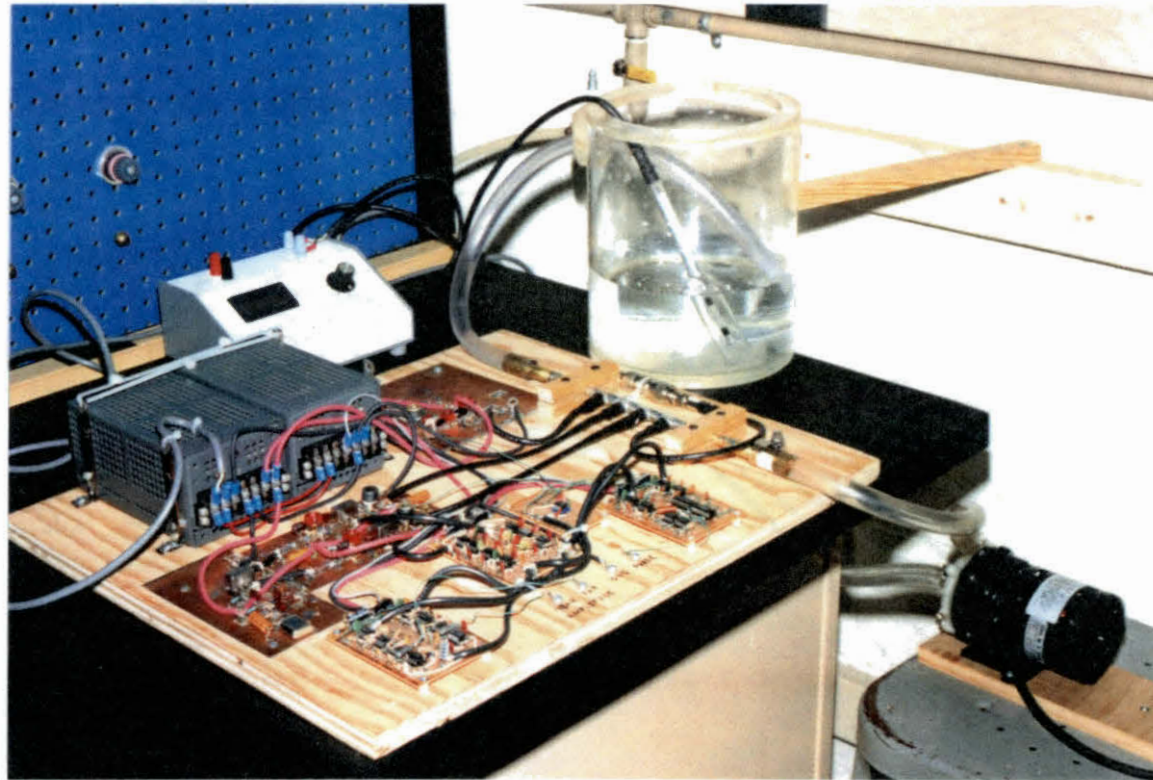


Figure 25. Measurement System Prototype

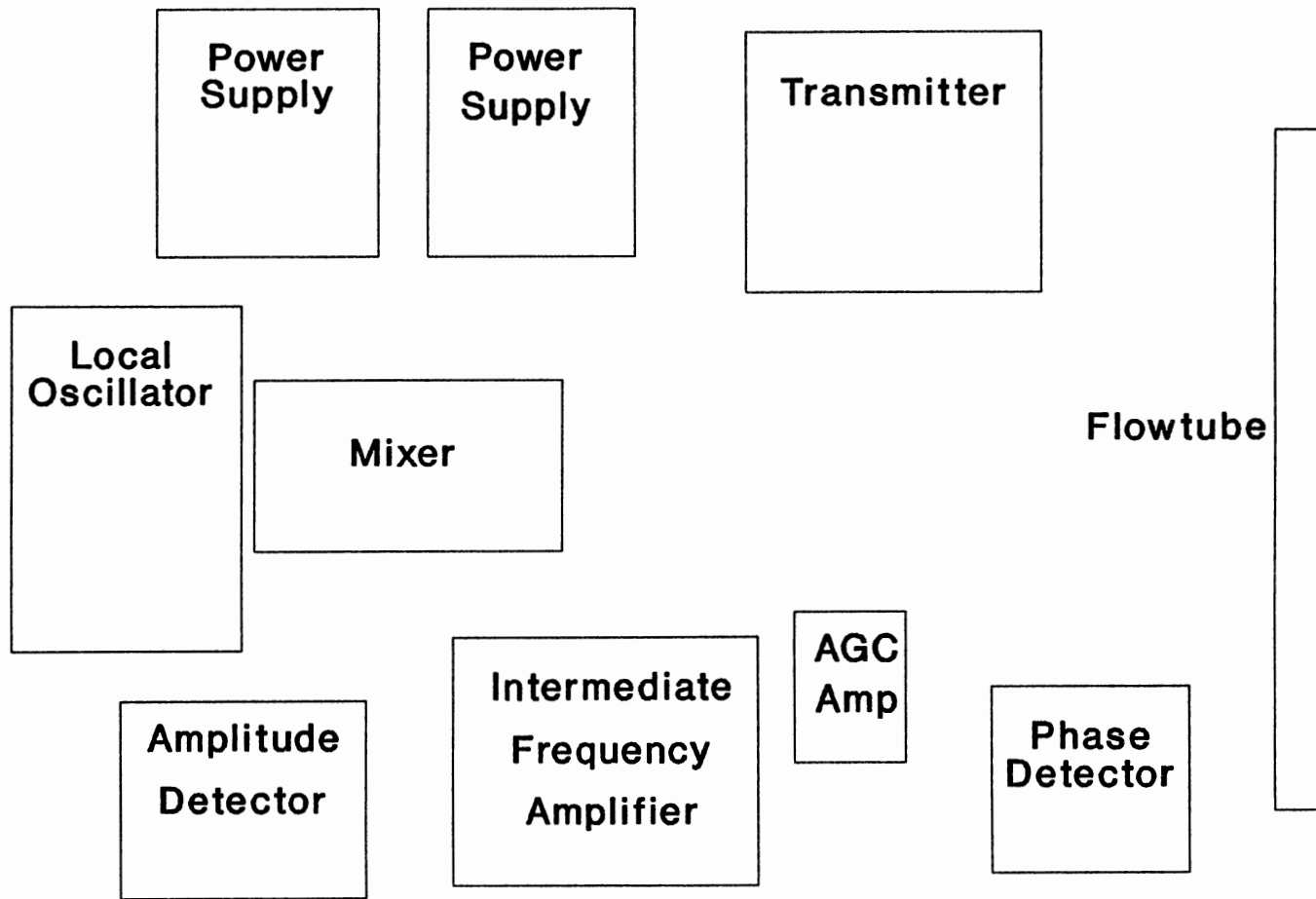


Figure 26. Measurement System Layout

CHAPTER VIII

PROTOTYPE TESTING

Introduction

Testing was carried out on the prototype flowtube with the network analyzer and then repeated using the prototype electronics. A flow loop was constructed with a fluid holding tank from which the fluid conductivity was controlled and monitored. Conductivity was varied by increasing the sodium chloride content. Fluid was pumped from the holding tank through the prototype flowtube and back into the holding tank. For the first set of tests, an output from the network analyzer was used to drive the flowtube transmission line while the phase shift and attenuation was measured at the analyzer inputs. The fluid conductivity was varied from approximately .05 to 33 mho/meter. Using sodium-chloride-saturated water, the temperature must be increased to approximately 140°F to achieve this conductivity range. Increasing the temperature above 140°F would exceed the temperature rating of the Yellowstone Instruments conductivity cell. The second test consisted of starting with a known volume of fluid with a fixed conductivity and then slowly adding known volumes of oil. Phase shift and attenuation were then measured as a function of oil volume.

After the tests with the network analyzer were completed, they were then repeated using the prototype electronics.

Phase and Attenuation Measurements

Figures 27 and 28 are plots of phase shift and attenuation versus the conductivity predicted by the theory, measured by the network analyzer, and measured by the prototype electronics. The same flowtube transmission line was used in both experimental measurements.

The network analyzer measurements of phase shift and attenuation are in good agreement with the theoretical curve at all but the smallest conductivities. The attenuation measurements made with the prototype electronics are in good agreement with the theoretical curve and network analyzer measurements at conductivities below about 15 mho/meter. Beyond that point, the attenuation measurements exhibit little or no change. Phase shift measurements from the prototype electronics are in good agreement with theoretical predictions out to approximately 11 mho/meter. Beyond this point they rise above the theoretical result. Testing showed that the individual phase shift and amplitude detectors give good results well beyond the limits reached in the flowloop test. However, the mixer board showed strong cross coupling between channels for low level signals on the far receiver, as evidenced by the changes induced by shielding lines and components on the mixer board. Unfortunately, the severe cross coupling brought on by the open air construction

techniques was unexpected and has significantly abbreviated the useful operating range of the prototype electronics. Placing the transmitter, local oscillator, and mixer in separate enclosures will significantly reduce cross coupling effects.

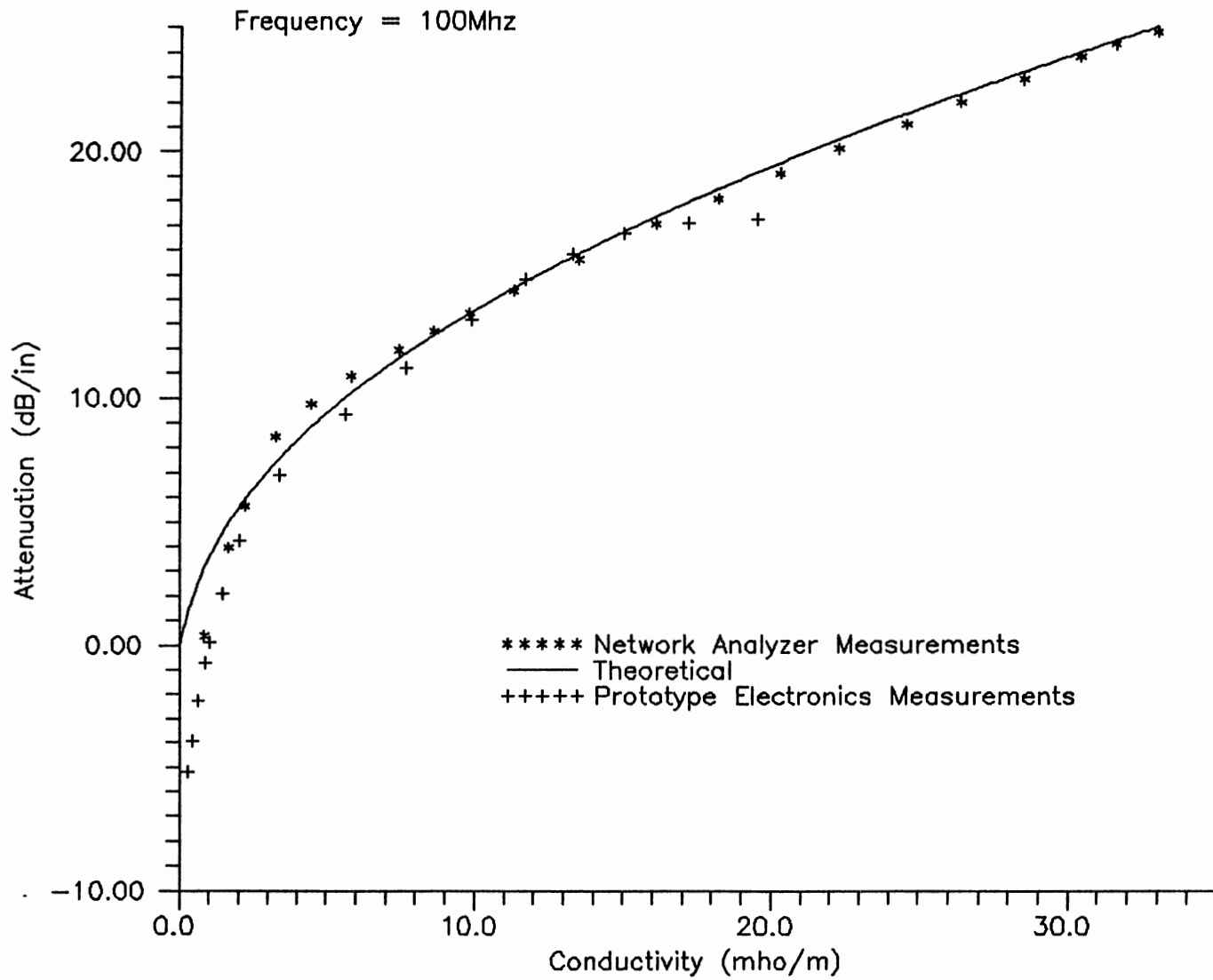


Figure 27. Attenuation For Final Flowtube Assembly

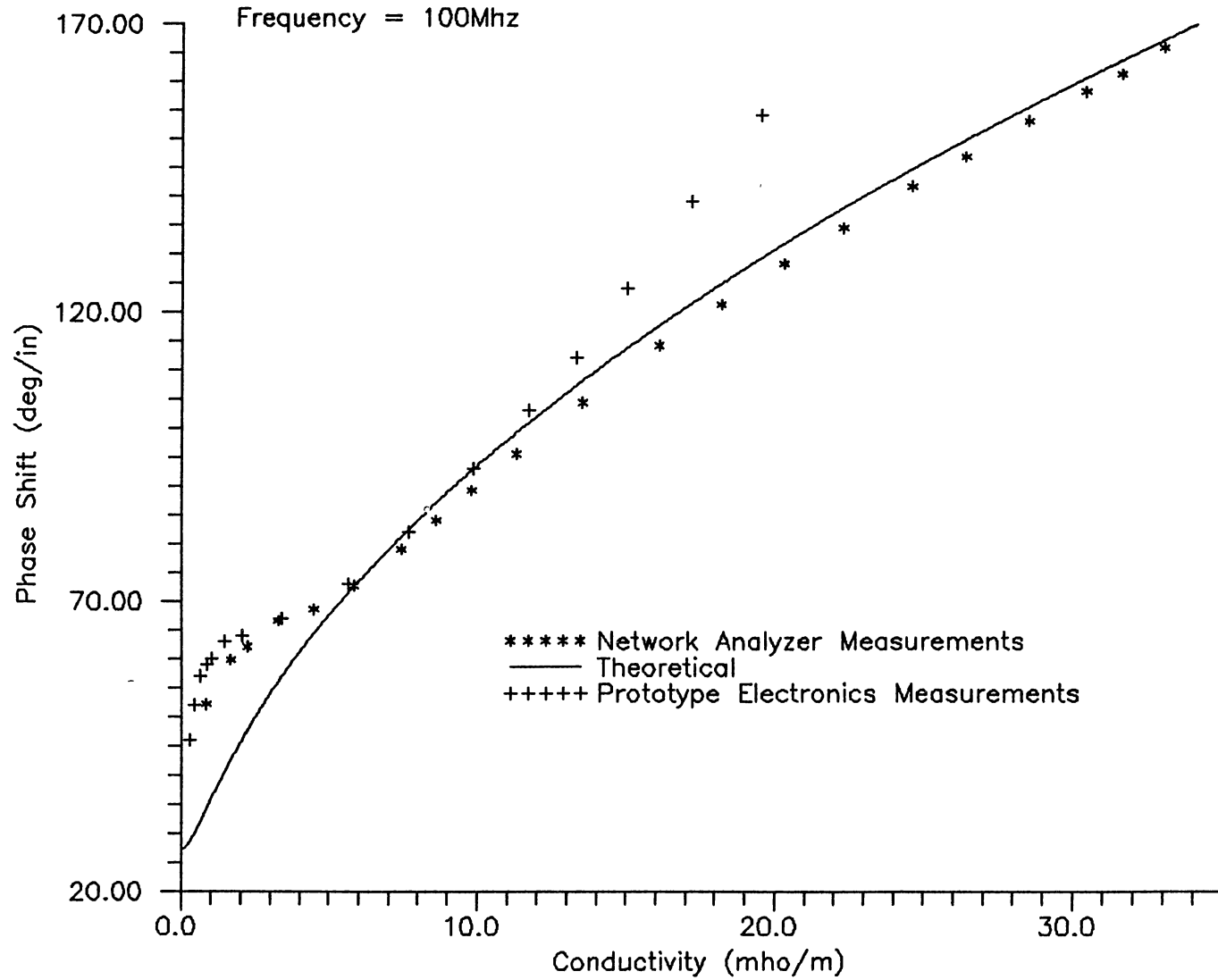


Figure 28. Phase Shift For Final Flowtube Assembly

Oil Volume Measurements

The first test in this series was performed using the prototype flowtube transmission line in the flowloop with the network analyzer providing the signal source and receiver processing. The initial fluid consisted of a known volume of water whose conductivity was 11.15 mho/meter. Incremental volumes of silicon oil were added and the phase shift and attenuation were measured. The results are plotted in Figures 29 and 30. The response for both measurements are approximately linear for mixtures ranging from 0 to 35% oil. At higher oil concentrations the measurement becomes somewhat erratic. Observation of the flowloop indicates a steady decrease in flow velocity as the oil volume increases. Above 35 percent oil concentrations, the flow velocity is not high enough to maintain a homogeneous mixture in the flowloop.

In the second set of tests, modifications in flowloop plumbing were made to remove restrictions in the flowloop that increased overall flow velocity. The test procedures were reversed so that a known volume of oil was placed in the flowloop and incremental volumes of water of consistent conductivity were added. The procedure was reversed in order to start with high oil volumes. This series of tests was run with the prototype electronics. The procedure was carried out for both 10 mho/meter and 2 mho/meter conductivity water. Figures 31 through 34 show the results. Again, this measurement was plagued by an inability to maintain a homogeneous mixture in the flowloop. The response is

approximately linear over some ranges, although inconsistencies are observed even with higher concentrations of water. With the increased flow volume, the linear response region was extended to approximately 50 percent oil concentration, but another problem was created on the low oil volume end. With the increased flow volume it was difficult to avoid air entrainment into the flowloop which also yields erratic measurements.

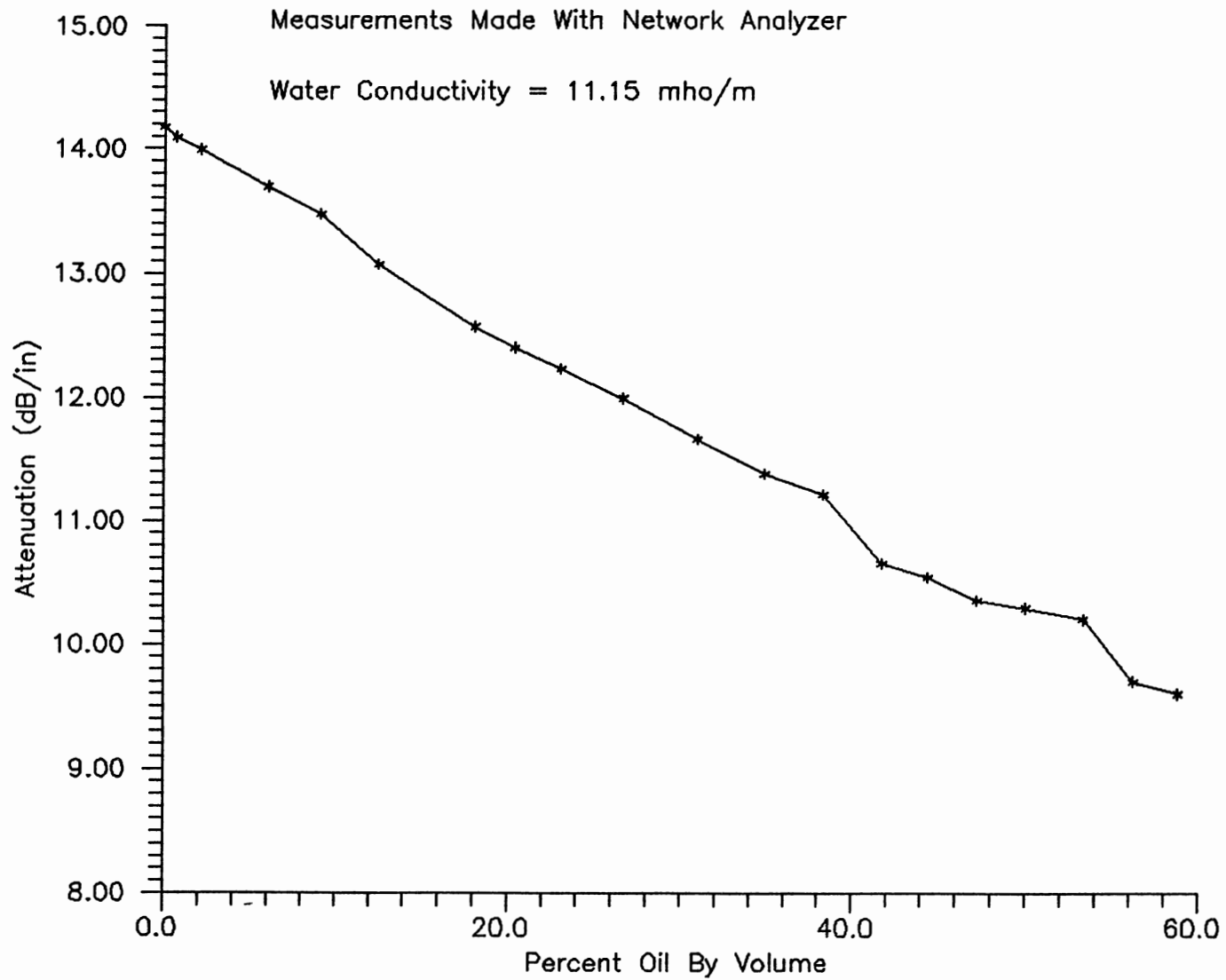


Figure 29. Measured Attenuation Versus Oil Volume

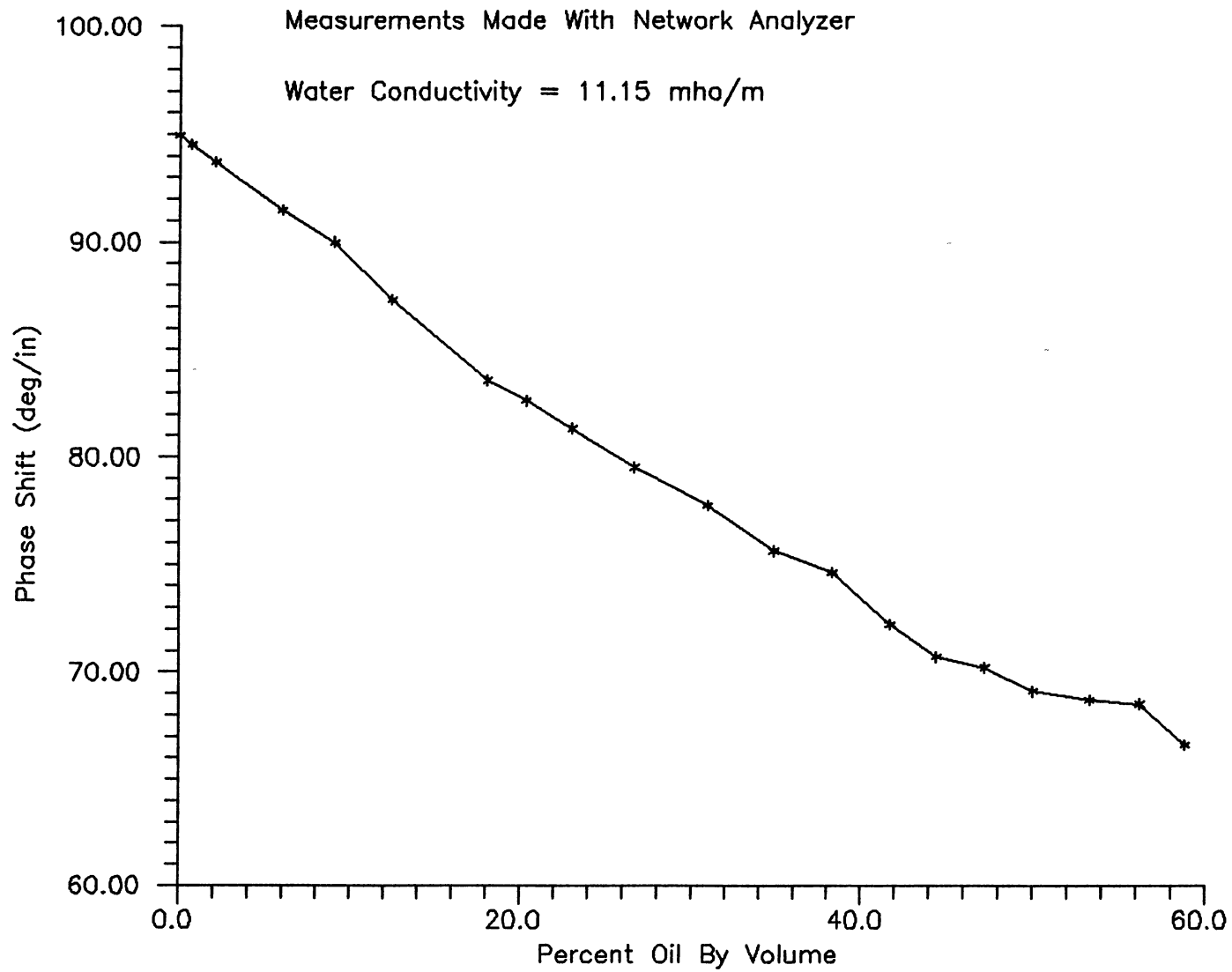


Figure 30. Measured Phase Shift Versus Oil Volume

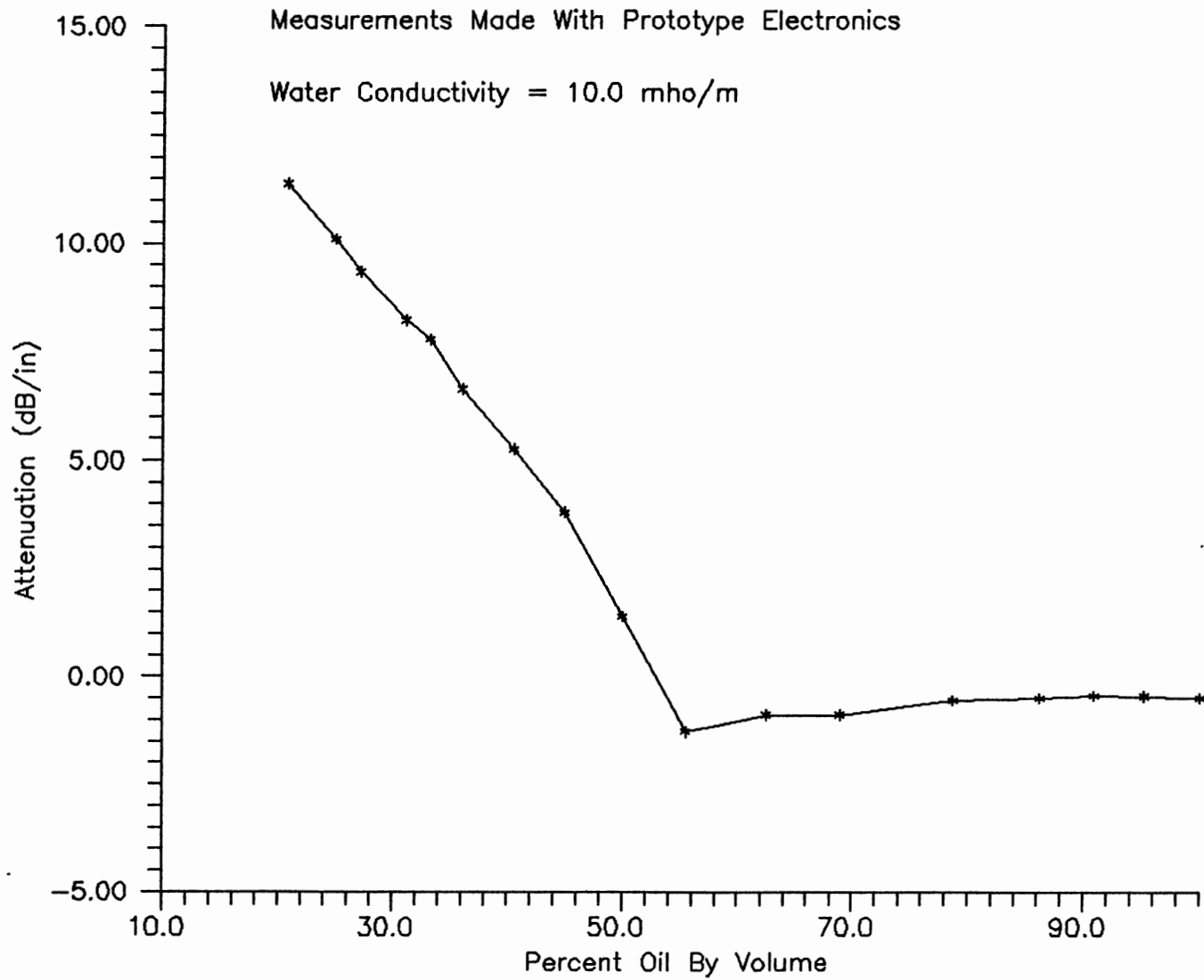


Figure 31. Measured Attenuation Versus Oil Volume

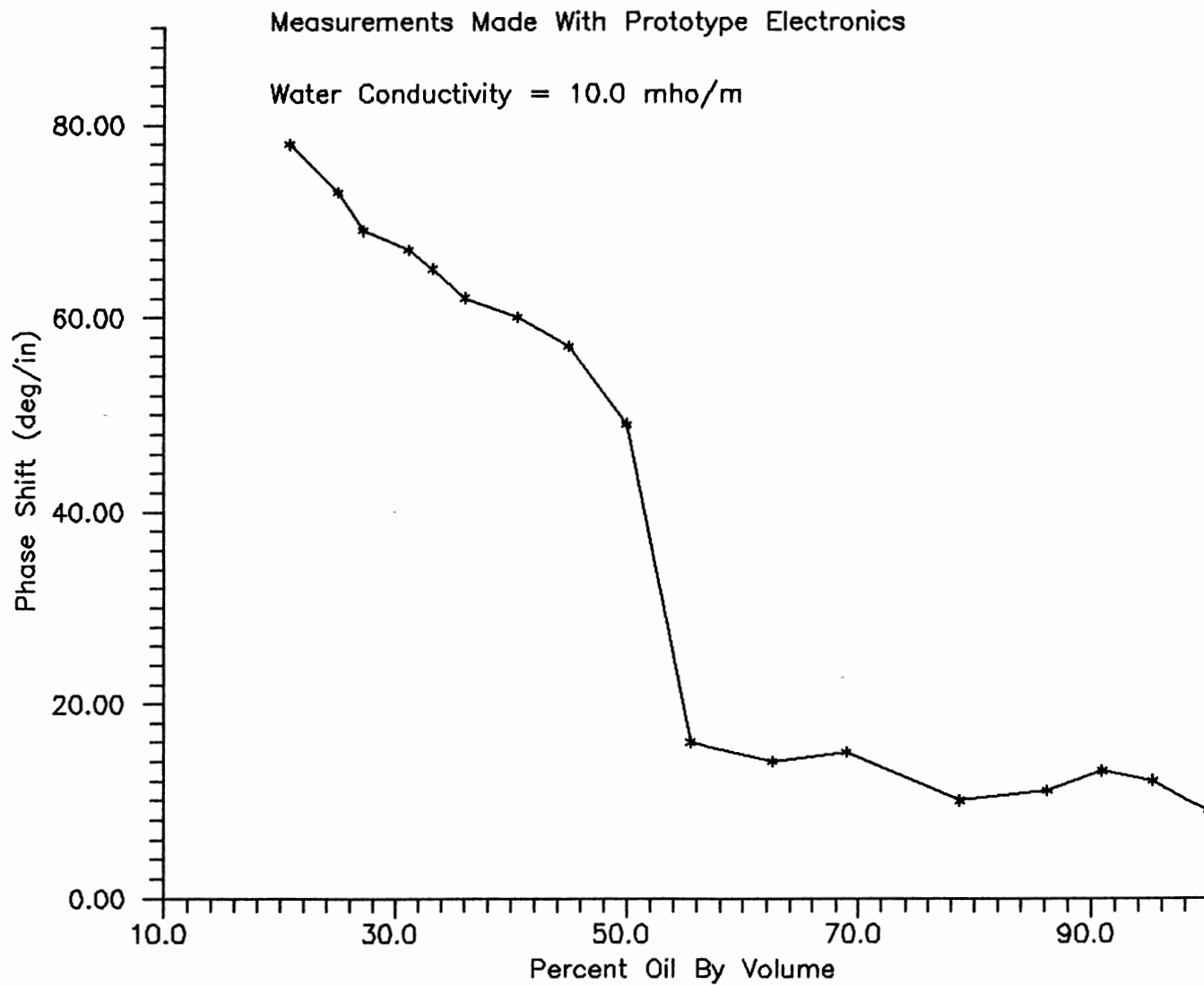


Figure 32. Measured Phase Shift Versus Oil Volume

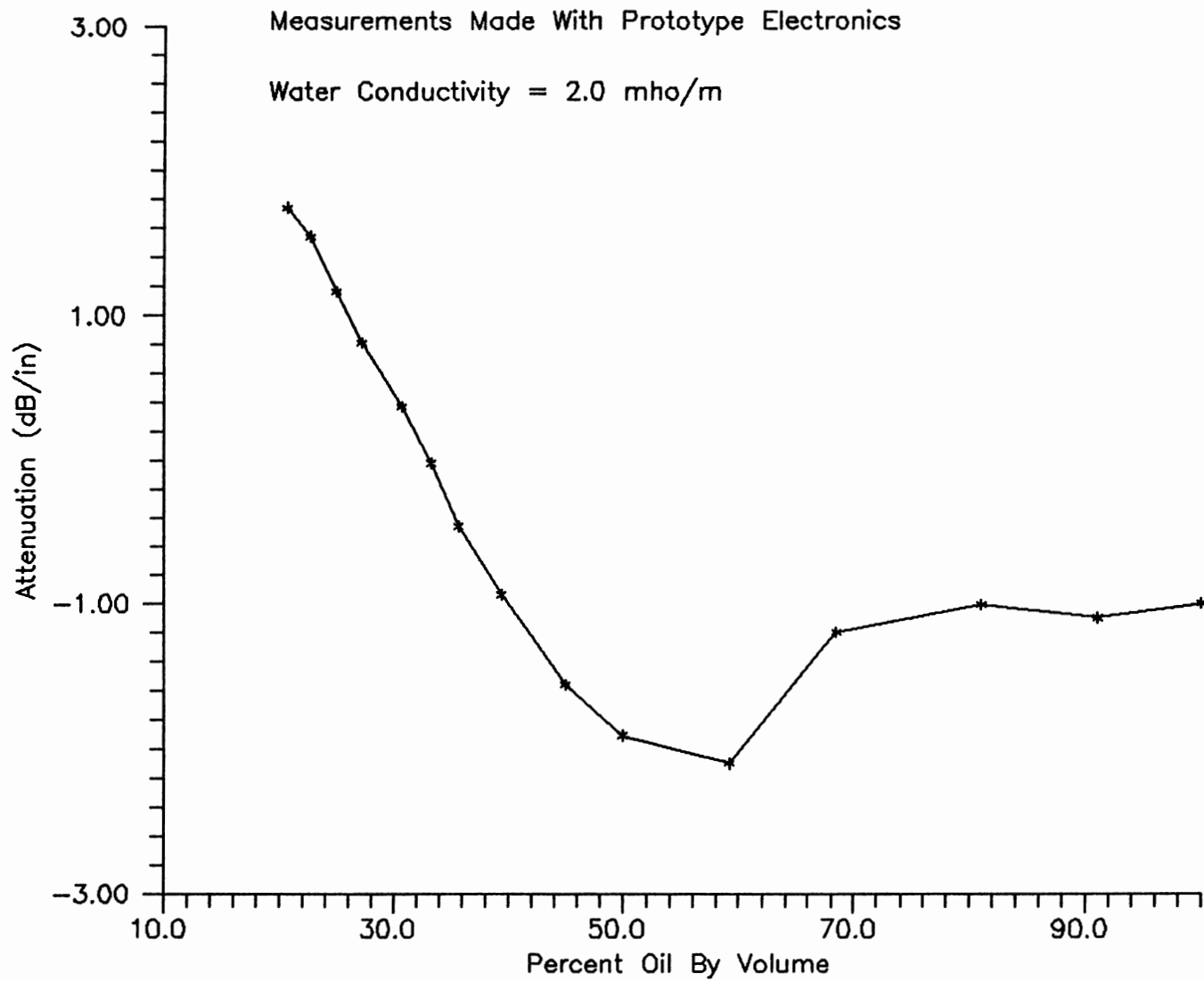


Figure 33. Measured Attenuation Versus Oil Volume

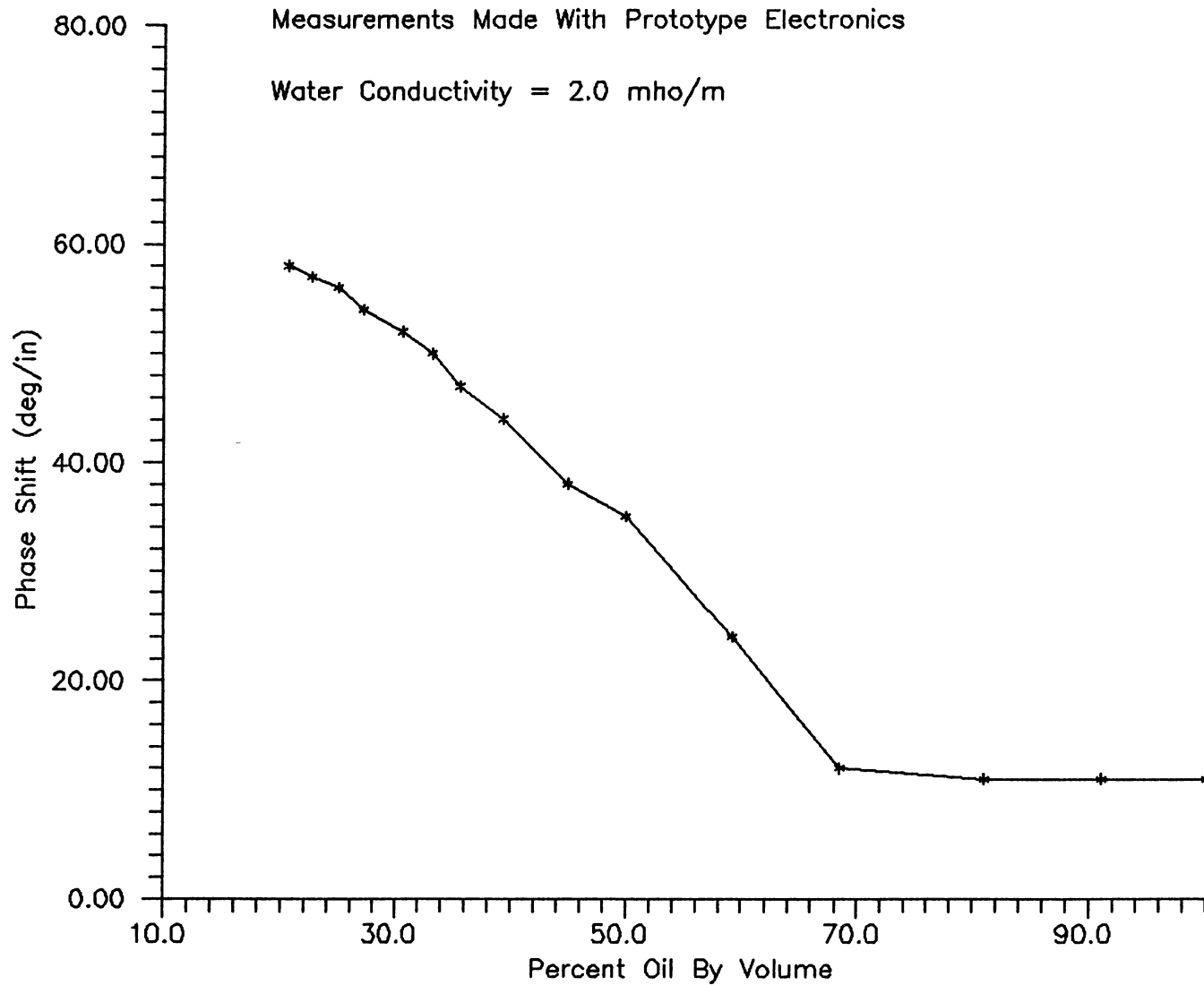


Figure 34. Measured Phase Shift Versus Oil Volume

CHAPTER IX

CONCLUSIONS AND COMMENTS

The primary objective of this project was to design, build, and test a fluid conductivity measurement system. The measurement of conductivity was to be made under dynamic fluid flow conditions while also estimating the hydrocarbon content of the fluid sample when possible.

The basic goals in the design and construction of this measurement system have been met. The measurement of fluid conductivity was accomplished under dynamic fluid flow conditions although testing was not completed over all of the specified conductivity range. A heated pressurized flowloop will be required to reach the maximum specified conductivity. Hydrocarbon content of a fluid sample can be measured for hydrocarbon content between 0 and 50 percent given some previous knowledge of fluid conductivity. The measurements made on samples with hydrocarbon content greater than 50 percent were inconclusive. These inconclusive measurements appear to be due to difficulties in maintaining a homogeneous mixture in the flowloop, not due to a limitation of the measurement technique itself.

The prototype electronics suffered from cross coupling between the transmitter, local oscillator, and mixer

sections. This cross coupling further abbreviated the range of conductivities over which measurements could be made.

Several problems remain to be resolved in future development of this system. An improved system should have the transmitter, local oscillator, and mixer electronics individually enclosed to alleviate the severe cross coupling experienced with this prototype electronics system. A heated, pressurized flowloop should also be constructed with a conductivity probe in the flowloop to verify operation at the maximum expected conductivity. Finally, some research into the flow dynamics of oil-water mixtures and their effects on the measurement system should be conducted.

A SELECTED BIBLIOGRAPHY

- [1] Atlas Wireline Services Log Interpretation Charts,
Houston, Texas
- [2] Design of Crystal and Other Harmonic
Oscillators, Benjamin Parzen, John Wiley
- [3] Coaxial Line Reflection Methods for Measuring Dielectric
Properties of Biological Substances at Radio
Frequencies - A Review, Maria A. Stuchly and
Stanislaw S. Stuchly, "IEEE Transactions on
Instrumentation and Measurement", Vol. IM-29, No. 3,
September 1980
- [4] Foundations for Microwave Engr., R.E. Collin, McGraw-
Hill, 1966
- [5] Applied Electromagnetism, Shen & Kong, PWS, 1987
- [6] Advanced Engineering Electromagnetics, Constantine A.
Balanis, John Wiley, 1989
- [7] George Dakermadjji and William T. Joines, A New Method
for Measuring the Electrical Properties of Sea Water
and Wet Earth at Microwave Frequencies, "IEEE
Transactions on Instrumentation and Measurement",
Vol. IM-26, No. 2, June 1977
- [8] Andrzej Korneta and Andrzej Milewski, The Application of
Two- and Three-Layer Dielectric Resonators to the
Investigation of Liquids in the Microwave Region,
"IEEE Transactions on Instrumentation and
Measurement", Vol. 37, No. 1, March 1988
- [9] Andrzej W. Kraszewski, Tian-Su You and Stuart Nelson,
Microwave Resonator Technique for Moisture Content
in Single Soybean Seeds, "IEEE Transactions on
Instrumentation and Measurement", Vol. 38, No. 1,
February 1989
- [10] H.M. Hafez, Walter Chudobiak and James S. Wight, The
Attenuation Rate in Fresh Water at VHF Frequencies,
"IEEE Transactions on Instrumentation and
Measurement", Vol. IM-28, No. 1, March 1979

- [11] N. Marcuvitz, Waveguide Handbook, McGraw-Hill, 1951
- [12] Juan R. Mosig, Jean-Claude E. Besson, Marianne Gex-Fabry and Fred E. Gardiol, Reflection of an Open-Ended Coaxial Line and Application to Nondestructive Measurement of Materials, "IEEE Transactions on Instrumentation and Measurement", Vol. IM-30, No. 1, March 1981
- [13] Devendra Misra, Mohinder Chhabra, Benjamin R. Epstein, Mark Mirotznik, and Kenneth R. Foster, NonInvasive Electrical Characterization of Materials at Microwave Frequencies Using an Open Ended Coaxial Line: Test of an Improved Calibration Technique, "IEEE Transactions on Instrumentation and Measurement", Vol. IM-38, No. 1, January 1990
- [14] Sushil K. Aggarwal and Ronald H. Johnston, Oil and Water Content Measurement of Sandstone Cores Using Microwave Measurement Techniques, "IEEE Transactions on Instrumentation and Measurement", Vol. IM-35, No. 4, December 1986
- [15] Walter J. Chudobiak, Barry A. Syrett, and H.M. Hafez, Recent Advances in Broad-Band VHF and UHF Transmission Line Methods for Moisture Content and Dielectric Constant Measurement, "IEEE Transactions on Instrumentation and Measurement", Vol. IM-28, No. 4, December 1979

VITA

Robert Michael Taylor
Candidate for the Degree of
Master of Science

Thesis: FLUID CHARACTERIZATION USING A TEM TRANSMISSION LINE

Major Field: Electrical Engineering

Biographical:

Personal Data: Born in Oklahoma City, Oklahoma January 26, 1958, the son of Robert H. and Barbara I. Taylor.

Education: Graduated from Chandler High School, Chandler, Oklahoma, in May 1976; received Bachelor of Science Degree in Electrical Engineering from Oklahoma State University, Stillwater, Oklahoma, May 1981; completed requirements for the Master of Science Degree at Oklahoma State University in December 1992.

Work Experience: Electronics Technician, School of Mechanical and Aerospace Engineering, Stillwater, Oklahoma, August 1990 to present.

Electrical Engineer, Atlas Wireline Services, Houston, Texas, May 1981 to August 1990.